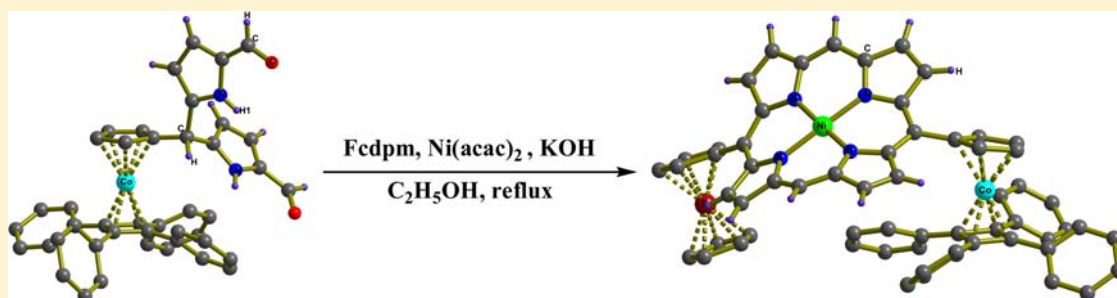


Synthesis, Spectral, and Structural Studies of Porphyrins Having Sterically Hindered [η^5 -CpCo(η^4 -C₄Ph₄)] Cobalt Sandwich Units at the Meso Positions

Karunesh Keshav, Dheeraj Kumar, and Anil J. Elias*

Department of Chemistry, Indian Institute of Technology, Delhi, Hauz Khas, New Delhi, 110016, India

S Supporting Information



ABSTRACT: Synthesis, spectral, and structural studies of the first examples of porphyrins substituted at the *meso* positions with sterically hindered η^5 -CpCo(η^4 -C₄Ph₄) cobalt sandwich units are described. The novel dipyrromethane derived cobalt sandwich compound $\{\eta^5-[(C_4H_4N)_2CH]C_5H_4\}Co(\eta^4-C_4Ph_4)$ **1**, as well as its parent aldehyde, $\eta^5-[C_5H_4(CHO)]Co(\eta^4-C_4Ph_4)$, were used in the synthesis of porphyrins having one or two η^5 -CpCo(η^4 -C₄Ph₄) groups at their *meso* positions. 1,9-Diformyldipyrromethane derived η^5 -CpCo(η^4 -C₄Ph₄) **2** was synthesized using dipyrromethane **1** under Vilsmeier conditions. A reaction of **2** with unsubstituted dipyrromethane under basic conditions in the presence of Pd(C₆H₅CN)₂Cl₂ yielded an A-type palladium coordinated porphyrin **3** [where A = η^5 -CpCo(η^4 -C₄Ph₄)]. A similar reaction of **2** with *meso* aryl and ferrocenyl-substituted dipyrromethanes yielded *trans*-AB type palladium coordinated porphyrins **4–6** [where A = η^5 -CpCo(η^4 -C₄Ph₄) and B = 4-*tert*-butylphenyl **4**, ferrocenyl **5**, and pentafluorophenyl **6**]. Reactions of **2** with 5-ferrocenyl dipyrromethane under the same reaction conditions in the presence of Ni(acac)₂ and Zn(OAc)₂ gave the trimetallic nickel(II) and zinc(II) complexed *trans*-AB type porphyrins **7** and **8** having both cobalt and iron sandwich units at the *meso* positions. Crystal structure of the Pd(II) porphyrin **5** and nickel(II) porphyrin **7** showed nonplanar structures having distinct ruffle type distortion of the porphyrin ring. Demetalation of the zinc(II) *trans*-AB type porphyrin **8** in the presence of trifluoroacetic acid gave the metal free base porphyrin **9**. Reactions of the cobalt sandwich aldehyde [$(\eta^5-C_5H_4(CHO))Co(\eta^4-C_4Ph_4)$] with sterically hindered dipyrromethane derivatives under acid-catalyzed condensation reactions gave *trans*-A₂B₂ type porphyrins [where A = η^5 -CpCo(η^4 -C₄Ph₄) and B = pentafluorophenyl, **10** mesityl **11**]. In contrast, reactions of [$\eta^5-C_5H_4(CHO)$]Co(η^4 -C₄Ph₄) with sterically unhindered *meso*-4-*tert*-butylphenyl dipyrromethane resulted in both AB₃ **12** and *cis*-A₂B₂ **13** type porphyrins [where A = η^5 -CpCo(η^4 -C₄Ph₄) and B = (4-*tert*-butylphenyl)] as a result of scrambling. The new porphyrin derivatives have been structurally characterized, and their spectral and electrochemical features were determined.

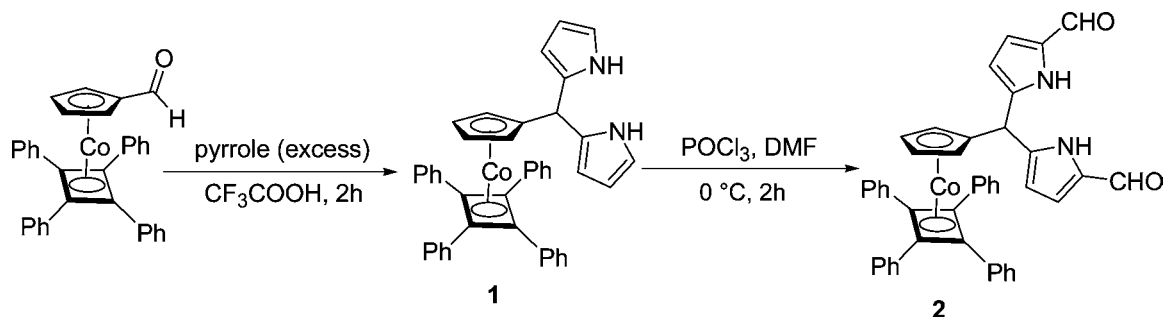
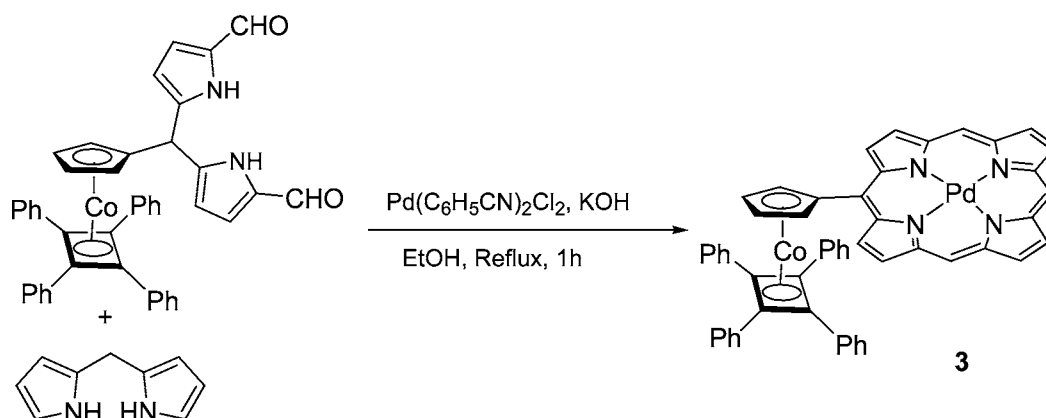
INTRODUCTION

Porphyrins substituted with ferrocene units at the periphery have attained considerable interest in recent years due to a range of potential applications.^{1,2} According to thermodynamic considerations, ferrocene substitution has the propensity to reduce singlet excited state of porphyrins making them potential candidates for developing photochemical devices which include donor–acceptor molecules which are mimics at the primary stages of photosynthesis.² Self-assembled monolayers on gold surfaces of ferrocene-derived porphyrins prepared by Lindsey and co-workers have been predicted to have application potential in information storage devices.³ The intervalence charge transfer bands shown by polyferrocenyl, polyphenyl porphyrins also indicate their utility in electronic

devices.⁴ Preparation of ferrocene-substituted porphyrins with or without a spacer group has therefore been an interesting offshoot of research in synthetic porphyrin chemistry. Ferrocene units directly attached to a porphyrin molecule at the *meso*-positions was first synthesized through an acid-catalyzed condensation reaction between ferrocene carboxaldehyde and pyrrole, which resulted in a number of products with low yields and poor selectivity.⁵ However Chandrashekar and co-workers, by using ferrocenyl dipyrromethane as a precursor, came up with a synthetic route to *meso* multiferrocene-substituted porphyrins with better selectivity and yields.⁶ Very

Received: May 3, 2013

Published: October 23, 2013

Scheme 1. Synthesis of the Dipyrromethane $\{\eta^5-[(C_4H_4N)_2CH]C_5H_4\}Co(\eta^4-C_4Ph_4)$ **1** and Its 1,9-Diformyl Derivative **2**Scheme 2. Synthesis of A-Type Porphyrin Having $\eta^5-CpCo(\eta^4-C_4Ph_4)$ at the Periphery

recently Senge et al. also developed a synthetic method based on Suzuki coupling between borylated porphyrins and ferrocene halides.⁷ Ferrocene-substituted porphyrins also have been synthesized with a variety of spacers between the ferrocene and porphyrin units.^{8–11}

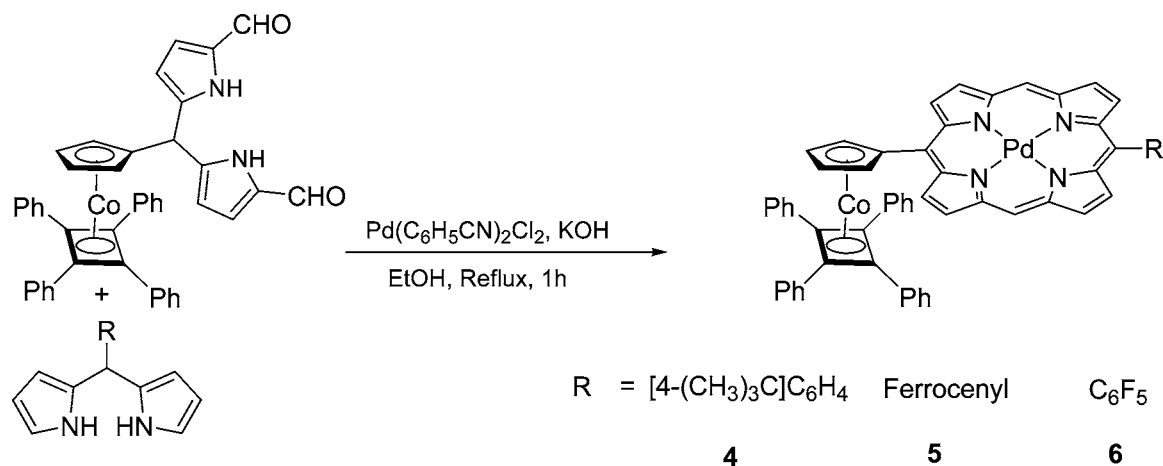
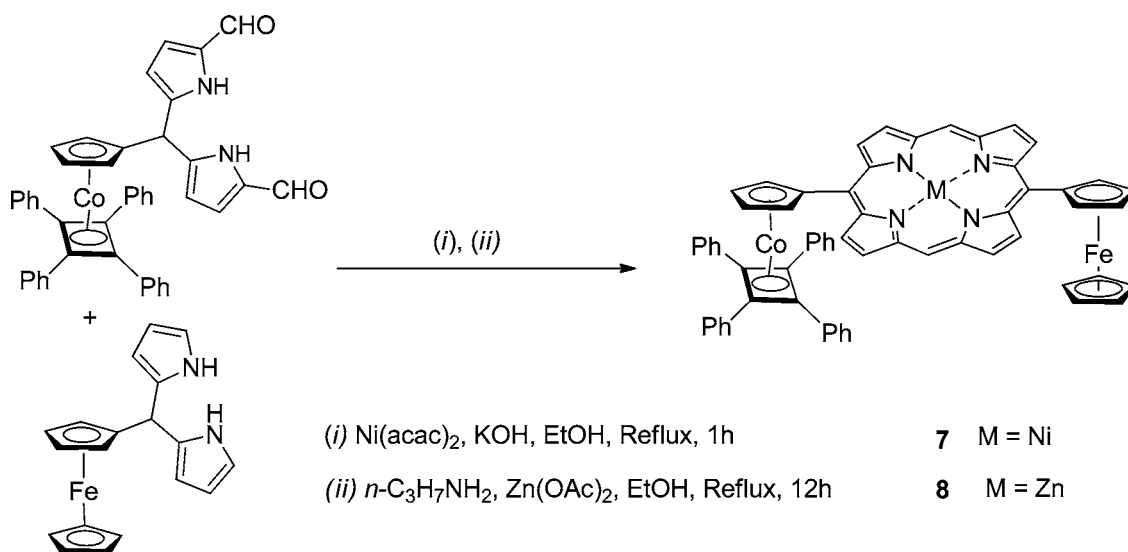
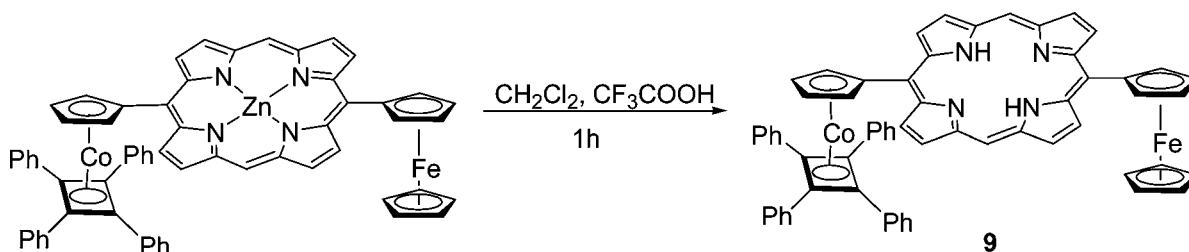
The 18-electron cobalt sandwich compound $\eta^5-CpCo(\eta^4-C_4Ph_4)$ is a highly air stable and sterically hindered molecule.¹² Compared to ferrocene, the cyclopentadienyl ring of this compound has been found to be very poorly reactive under standard metallocene derivatization procedures.¹³ However, we as well as others have been developing alternate methods to prepare novel derivatives of this highly stable and easy to handle cobalt sandwich compound.^{14–17} The basal bulkiness of $\eta^5-CpCo(\eta^4-C_4Ph_4)$ has resulted in the development of excellent chiral organometallic catalysts, while its electron donor capability has shown potential for realizing organic luminescent materials and photovoltaic devices.¹⁸ In this paper we report the synthesis and characterization of the first examples of $\eta^5-CpCo(\eta^4-C_4Ph_4)$ derived porphyrins by a base-catalyzed synthesis using the hitherto unknown dipyrromethane derivative of $\eta^5-CpCo(\eta^4-C_4Ph_4)$. We have for comparison also carried out acid-catalyzed reactions using the carboxaldehyde $\eta^5-[(C_5H_4(CHO))]Co(\eta^4-C_4Ph_4)$ with aryl dipyrromethane compounds to introduce more than one $\eta^5-CpCo(\eta^4-C_4Ph_4)$ unit on the porphyrin periphery. Although a few examples of non-ferrocenyl sandwich and half sandwich units have been incorporated on the porphyrin periphery, they have been mostly prepared by statistical methods which resulted in poor selectivity of products.¹⁹ The new porphyrins consisting of metal complexed and free base porphyrins with mono- and disubstitution of $\eta^5-CpCo(\eta^4-C_4Ph_4)$ at the periphery have been prepared by rational methods and

characterized by a variety of spectral, electrochemical, and structural studies.

RESULTS AND DISCUSSION

The hitherto unknown cobalt sandwich derived dipyrromethane **1** was prepared by the condensation of $\eta^5-[(C_5H_4(CHO))]Co(\eta^4-C_4Ph_4)$ with an excess of pyrrole in the presence of trifluoroacetic acid. Compared to analogous ferrocenyl dipyrromethane which was obtained in 78% yield, compound **1** was obtained in 87% yield.²⁰ The formylation of this dipyrromethane when carried out under Vilsmeier conditions ($POCl_3/DMF$) at $0\text{ }^\circ\text{C}$ afforded its 1,9-diformyl derivative **2** in 65% yield (Scheme 1).

The diformylated dipyrromethane **2** was used for the synthesis of an A-type porphyrin having at its *meso* positions just one cobalt sandwich unit. A-type of porphyrins are of special interest as they can act as precursors for making new AB, ABC, and ABCD types of multisubstituted porphyrins which are otherwise difficult to realize.²¹ They are also materials of interest due to their utility as reference compounds in physicochemical investigations such as perturbation studies.²¹ In spite of their application potential, synthetic routes to *meso*-substituted porphyrins with fewer substituents, particularly A-type of *meso*-monosubstituted, β -unsubstituted porphyrins were relatively unknown till 2002 when Senge and co-workers for the first time came up with a practical synthesis of such porphyrins.²² The A-type of free base porphyrins with substituents such as phenyl, *tert*-butyl, and ethyl-propyl at one of the *meso* positions have been reported using a [2 + 2 + 1] condensation of dipyrromethane, pyrrole-2-carboxaldehyde, and another aldehyde with yields varying from 2 to 12%.²¹ Although no reports are available in the literature on the synthesis of metal-sandwich derived A-type *meso*-monosub-

Scheme 3. Synthesis of Pd(II) Coordinated *trans*-AB-Type Porphyrins Having η^5 -CpCo(η^4 -C₄Ph₄) Unit at Their *meso* PositionsScheme 4. Synthesis of Ni(II) and Zn(II) Coordinated *trans*-AB Type PorphyrinsScheme 5. Synthesis of *trans*-AB Type Free Base Porphyrin

stituted, β -unsubstituted porphyrins, the molecular and electronic structure of ferrocene *meso*-substituted, A-type free base porphyrin has been predicted using density functional theory (DFT) and time-dependent density functional theory (TD-DFT) methods.²³

In contrast to the [2 + 2 + 1] condensation method by Senge et al., we have attempted a two-component template based rational method²⁴ involving *meso*-unsubstituted dipyrromethane and compound 2. Condensation reaction of 2 with dipyrromethane in the presence of Pd(C₆H₅CN)₂Cl₂, KOH, and ethanol as a solvent under reflux conditions gave the red-colored A-type porphyrin 3 in 18% yield (Scheme 2). This

synthetic approach provides scope for realizing more examples of metal coordinated A-type of porphyrins with different organometallic substituents.

Analogous reactions of 2 with aryl- and ferrocenyl-substituted dipyrromethanes under similar reaction conditions gave the *trans*-AB type porphyrins 4, 5, and 6 in 14, 24, and 10% yield, respectively (Scheme 3).

To observe the effect of the size of the metal ion on the spectral properties of the metal sandwich derived porphyrins, we used different metal ions such as Ni(II) and Zn(II) as templates in the synthesis. Condensation reaction of 2 with ferrocenyl dipyrromethane in the presence of Ni(acac)₂, KOH,

11 (Scheme 6). This observation is similar to what has been observed in the acid-catalyzed reaction of *p*-tolualdehyde with mesityl dipyrromethane which exclusively gave only the *trans* product.²⁷

Interestingly, the reaction of $[(\eta^5\text{-C}_3\text{H}_4\text{CHO})\text{Co}(\eta^4\text{-C}_4\text{Ph}_4)]$ with a sterically less hindered dipyrromethane 4-Bu^t-C₆H₄-[CH(C₄H₄N)₂] under similar reaction conditions gave AB₃ **12** and *cis*-A₂B₂ **13** type porphyrins which are products resulting from scrambling (Scheme 7). The formation of these compounds **12** and **13** can be explained by invoking acid-catalyzed fragmentation of a polypyrrane into pyrrolic and azafulvene components followed by their recombination which is well documented in the porphyrin literature.²⁷ Formation of the *cis*- $\eta^5\text{-CpCo}(\eta^4\text{-C}_4\text{Ph}_4)$ disubstituted compound **13** indicates that the steric bulkiness of the cobalt sandwich unit does not hinder the formation of *meso*-disubstituted porphyrin derivatives.

NMR Spectral Studies on Compounds 2–13. In the ¹H NMR, the disappearance of a signal at 6.44 ppm corresponding to 1,9-protons of dipyrromethane of **1** and appearance of a typical singlet at 10.44 ppm corresponding to an aldehydic proton indicated that formylation has occurred at these positions leading to compound **2**. In the ¹H NMR of compound **2**, all pyrrolic protons shifted downfield after formylation, due to the increased electron withdrawing nature of the formyl group. Similar downfield shifts have also been observed during conversion of *p*-tolylidipyrromethane to its 1,9-diformyl derivative.²⁸

The ¹H NMR spectra of the A-type porphyrin **3** showed two separate singlets having peak intensity in the ratio of 2:1 at 10.00 and 10.13 ppm respectively which can be assigned to protons at the *meso* positions. Two doublets corresponding to two protons each and one multiplet corresponding to four protons were observed in the range of 8.74–9.72 ppm for the β -pyrrolic hydrogens. A similar ¹H NMR peak pattern was observed in the case of *meso*-mesityl-substituted A-type of porphyrins in the range of 9.38–10.26 ppm.²⁹

Because of the presence of two different substituents at 5 and 15 positions, the *trans*-AB type porphyrins **4–9** showed four different sets of doublets corresponding to two each for β -pyrrolic hydrogens and one singlet corresponding to the two *meso* hydrogen atoms. The *trans*-AB type porphyrin **4** also showed four sets of doublets in the range of 8.79–9.76 and a singlet at 10.02 ppm. Unsubstituted cyclopentadienyl units of ferrocene in compounds **5** and **7–9** gave a singlet in the range of 3.92–4.30 ppm, while substituted cyclopentadienyl units were observed as two sets of signals in the range of 4.80–5.95 ppm. Nickel coordinated *trans*-AB porphyrin **7** showed four different sets of doublets in the range of 8.53–9.65 ppm and a singlet at 9.29 ppm. Similar to **5**, *trans*-AB porphyrin **6** also showed four different sets of doublets in the range of 8.79–9.77 and a singlet at 10.06 ppm. Demetalation of the zinc coordinated porphyrin **8** was easily monitored by the appearance of two broad peaks at –1.99 and –1.90 ppm corresponding to the ring –NH protons. After demetalation, chemical shift of the *meso* proton was also found to shift downfield significantly (from 9.61 to 10.06) in **9**.

¹H NMR of the $\eta^5\text{-CpCo}(\eta^4\text{-C}_4\text{Ph}_4)$ *trans*-disubstituted compounds **10** and **11** were easily differentiated from that of the *cis* isomer **13**. In contrast to the *trans*-substituted compounds which showed only two peaks in the pyrrolic region, the *cis* isomer showed four different peaks in the pyrrolic region which can be ascribed to the lower symmetry of

the latter. Two doublets observed at 8.05 and 9.38 ppm for four protons each correspond to two sets of β -pyrrolic hydrogens for the *trans*-A₂B₂ porphyrin **10**. This is similar to the observation in the case of the *trans*-A₂B₂ type ferrocene analogue [5,15-bisferrocenyl-10,20-bis-(pentafluorophenyl) porphyrin] where it was observed at 8.66 and 9.97 ppm.³⁰ Similarly, β -pyrrolic hydrogens of the other *trans* isomer **11** gave doublets at 8.04 and 9.36 ppm.

In contrast to the *trans* isomer, the *cis* isomer **13** showed four different peaks at 8.28, 8.65, 8.84, and 9.19 ppm. A similar peak pattern was observed in the case of its ferrocene analogue 5,10-bisferrocenyl-15,20-diphenyl porphyrin^{4a} where it was observed at 8.65, 8.71, 9.78, 9.90 ppm, respectively.

UV–vis Spectral Studies of Compounds 3–13. UV–vis spectra of the compounds **3–13** were recorded in dichloromethane, and the spectral data of compounds **4–9** and **10–13** are summarized in Figures 1 and 2, respectively. The spectra of

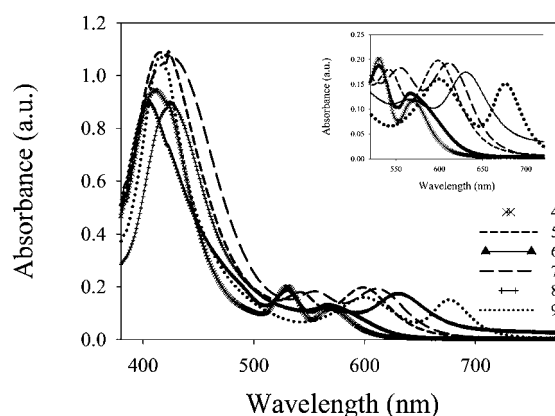


Figure 1. Electronic absorption spectra of *trans*-AB type compounds **4–9** in dichloromethane at 1×10^{-6} M.

A type porphyrin **3** is given in the Supporting Information. The effect of substitution of $\eta^5\text{-CpCo}(\eta^4\text{-C}_4\text{Ph}_4)$ units on the spectral properties of the porphyrin ring is clearly reflected in these studies. A-type porphyrin **3** showed the Soret absorption band at 406 nm. This absorbance is close to the absorption maxima at 406 nm reported in the case of the A-type zinc(II) coordinated 5-mesitylporphyrin.²⁹ The *trans*-AB type porphyrins **4–9** showed absorbance in the range of 411–423 nm which is close to the Soret absorption shown by the free base *trans*-AB type 5-ferrocenyl-15-phenyl porphyrin (424 nm).³¹ The palladium(II) *trans*-AB type porphyrin **5**, which has both ferrocene and the cobalt sandwich unit at its *trans* positions, showed absorption maxima at 416 nm. Among the *trans*-AB type porphyrin complexes, the nickel(II) porphyrin **7** showed a broad Soret absorption band at 423 nm (Figure 1). The broadening of this spectrum may be due to the distortion of the porphyrin macrocycle as evident from the highly ruffled nature of the porphyrin core which was confirmed from its molecular structure. Similar broadening of Soret absorption band was reported for the distorted Ni(II) tetra(*tert*-butyl)porphyrin.³² The zinc coordinated porphyrin **8** showed absorption at 422 nm while the same after demetalation (compound **9**) showed absorption at 417 nm.

The *trans*-A₂B₂ porphyrin **10** showed absorbance at 423 nm, which is similar to that of the reported 5,15-bisferrocenyl-10,20-bis-(pentafluorophenyl) porphyrin³⁰ which showed absorbance maxima at 424 nm (Figure 2). The AB₃ type porphyrin **12**

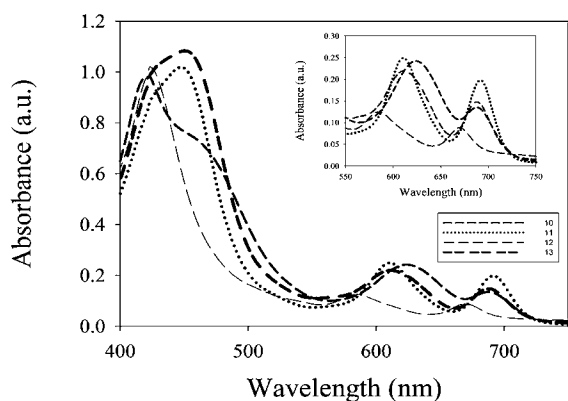


Figure 2. Electronic absorption spectra of A_2B_2 and AB_3 type compounds 10–13 in dichloromethane at 1×10^{-6} M.

[where B = (4-*tert*-butylphenyl)] having only one cobalt sandwich unit showed Soret absorbance at 423 nm and a Q-band at 581 nm, which is similar to the absorption maxima observed in the case of its ferrocene analogue, 5-ferrocenyl 10,15,20-tri-(4-*tert*-butylphenyl) porphyrin^{6a} for which these bands were observed at 423 and 510 nm respectively. However, further substitution of phenyl by cobalt sandwich unit resulted in a significant increase in the absorption maxima toward the higher wavelength region.

For instance, in contrast to the reported 5,10-diferrocenyl 15, 20-di(4-*tert*-butylphenyl) porphyrin^{6a} which showed absorption at 426 nm, for both *trans*- A_2B_2 porphyrin 11 and *cis*- A_2B_2 porphyrin 13, absorption shifted more toward the red region. Both compounds showed absorption maxima at 443 nm for the Soret band and Q bands at 610 and 612 nm for 12 and 13 respectively (Figure 2). This red-shift in both Soret and Q bands is probably due to the increased nonplanarity of the porphyrin core after replacement of one of the phenyl groups by η^5 -CpCo(η^4 -C₄Ph₄). This observation was similar to the reported absorption spectra for ferrocene-substituted porphyrins where also the position of absorption band maxima was found to depend on the extent of ferrocene substitution on the porphyrin.^{6a}

Red shifts of Soret and Q-bands in the UV–visible spectrum of ferrocene-substituted porphyrins were reported relative to the parent tetraphenyl porphyrin.^{6a} However, effect of the cobalt sandwich unit on the variation in absorption maxima was found to be even more pronounced. For example, compound 12, where only one η^5 -CpCo(η^4 -C₄Ph₄) is attached to the porphyrin ring, showed absorbance maxima (Soret band) at 423 nm, while for the η^5 -CpCo(η^4 -C₄Ph₄) *trans*-disubstituted compound 11, the Soret absorption maxima increased from 423 to 443 nm. Similar variation on going from mono- to diferrocene substitution indicated only a small increment in the position of the Soret absorption band (423–426 nm).^{6b}

X-ray Crystal Structures of Compounds 1, 2, 3–5, 7, 9, 11, and 13. The crystal structures of compounds 3–5, 7, 9, 11, and 13 are given in Figures 3–9, and those of compounds 1 and 2 are given in the Supporting Information. From the crystal structure of compound 1, it was observed that the average C–C bond distance of cyclopentadienyl ring 1.415(1) Å and the average bond angle 107.99(4)° were in good agreement with bond lengths and angles for the related compound (η^5 -cyclopentadienyl)(η^4 -1,3-diferrocenyl)-(2,4-diphenylcyclobutadiene)cobalt.³³ The crystal structure of the 1,9-diformyl derivative 2 showed the occurrence of two

molecules of solvent (chloroform) within the asymmetric unit. The bond lengths and bond angles after formylation of the cobalt sandwich unit remained nearly the same as that of compound 1.

Nonplanar distortions of the porphyrin macrocycle depend on factors such as the number, position, size, and shape of the peripheral substituents and the size of metal ions present³⁴ at the center of the porphyrins. In general, the present study indicates that the bulky substituent η^5 -CpCo(η^4 -C₄Ph₄) at the *meso* position plays a significant role in deciding the planarity of the porphyrin macrocycle. While some examples of aryl and alkyl based A-type porphyrins are known in the literature,^{21,22} examples whose crystal structure have been determined are very few in number.³² A literature search on A-type of porphyrins indicates only one known example of ferrocene *meso*-substituted derivative which is actually an octamethylporphyrin.³⁵ The η^5 -CpCo(η^4 -C₄Ph₄) *meso*-substituted porphyrin 3 to the best of our knowledge is the first example of a structurally characterized metal sandwich derived A-type porphyrin.

Porphyrin unit of 3 shows a saddle type, out-of-plane distortion with some contribution of wave type distortion. This deviation from planarity seems to be a result of localized influence of the cobalt sandwich substituent η^5 -CpCo(η^4 -C₄Ph₄) present at its *meso* position (Figure 3). The tilt angle of

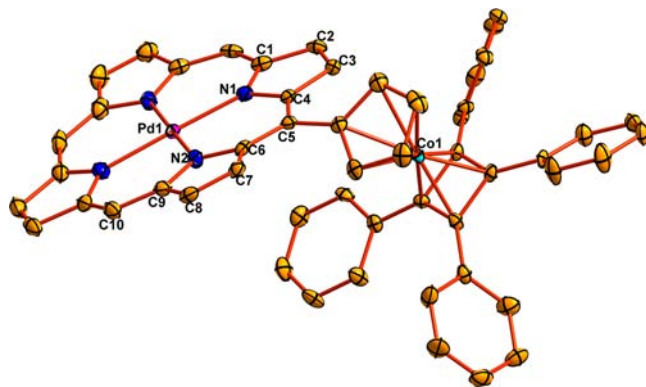


Figure 3. Molecular structure of A-type porphyrin 3. Thermal ellipsoids are drawn at the 30% probability level. All hydrogen atoms are omitted for clarity. Selected bond lengths (Å) and angles (deg) with esd's in parentheses: C(1)–C(2) 1.433(8); C(2)–C(3) 1.333(7); C(3)–C(4) 1.451(7); Pd(1)–N(1) 2.010(4); C(1)–C(2)–C(3) 107.0(5); C(2)–C(3)–C(4) 108.6(5); C(4)–C(5)–C(6) 121.9(5).

the individual pyrrole rings with respect to the mean plane passing through all the 24 ring atoms are 6.9, 4.9, 3.8, and 4.1°. The *meso* carbon atom which is attached to the cobalt sandwich unit has been found to be 0.11 Å away from the mean plane defined by all the 24 atoms of porphyrin unit (Figure 10A).

This is in contrast to the reported structure of the Ni(II) coordinated *tert*-butyl-substituted A-type porphyrin which showed a significant ruffle type of distortion.³² The extent of out-of-plane distortion is less in the case of 3, and the displacement of each atom from the mean plane defined by the porphyrin ring has been found to vary in the range of –0.203 to 0.268 Å (Figure 10A). The dihedral angle between the cyclopentadienyl ring and the mean plane defined by the porphyrin ring was found to be 33.7(2)°. The macrocycle shows only a small in-plane distortion, and the core elongation parameter was found to be 0.080 Å.

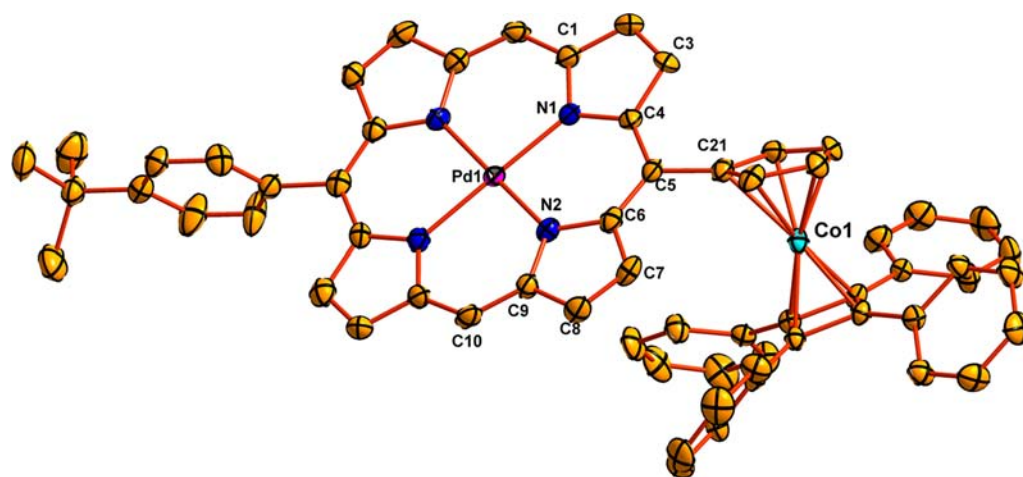


Figure 4. Molecular structure of the AB-type porphyrin 4. Thermal ellipsoids are drawn at the 30% probability level. All hydrogen atoms are omitted for clarity. Selected bond lengths (Å) and angles (deg) with esd's in parentheses C(1)–C(2) 1.417(9); C(2)–C(3) 1.337(9); C(3)–C(4) 1.433(8); N(1)–C(1) 1.379(7); Pd(1)–N(1) 2.007(5); C(6)–C(5)–C(4) 123.1(6); C(9)–C(10)–C(11) 126.6(6).

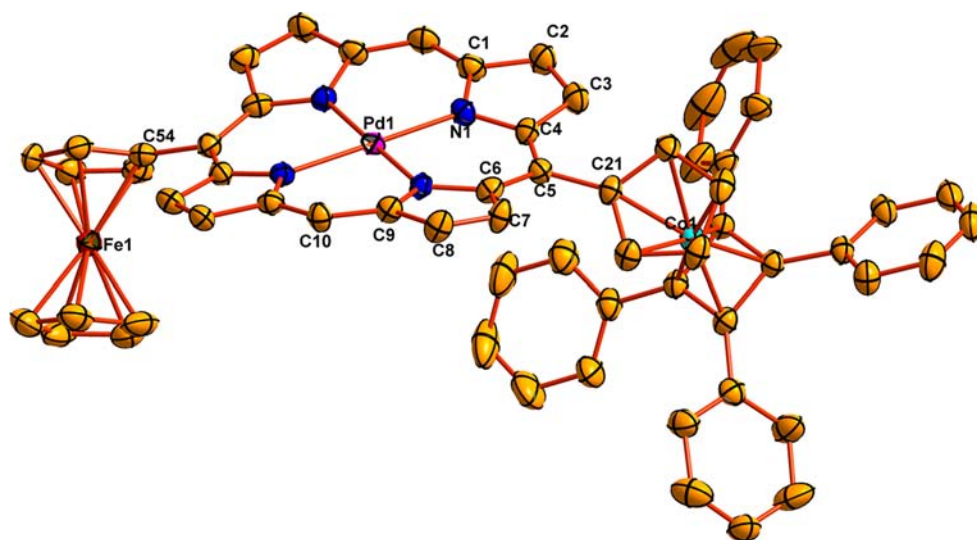


Figure 5. Molecular structure of the *trans*-AB-type porphyrin 5. Thermal ellipsoids are drawn at the 30% probability level. All hydrogen atoms are omitted for clarity. Selected bond lengths (Å) and angles (deg) with esd's in parentheses C(1)–C(2) 1.417(6); C(2)–C(3) 1.327(7); C(3)–C(4) 1.427(6); N(1)–C(1) 1.368(5); Pd(1)–N(1) 2.015(3); C(4)–C(5)–C(6) 121.9(4); C(11)–C(10)–C(9) 125.9(4).

The crystal structure of the *trans*-AB type compound 4 (Figure 4) similar to 3 shows a saddle type of distortion, and the effect of substitution of the *tert*-butylphenyl group at its *meso* position, *trans* to the cobalt sandwich unit, does not seem to affect the nature of distortion. This type of out-of-plane distortion is in contrast to the ruffle type of distortion reported for the structure of the *trans*-AB type 5-ferrocenyl-15-phenyl porphyrin.³¹ The *meso* carbon atom attached to the cobalt sandwich unit has been found to be 0.14 Å away from the mean plane defined by all the 24 atoms of the porphyrin unit (Figure 10B).

In the structure of 4, the dihedral angles between the cyclopentadienyl ring and the benzene moiety of the *meso-tert*-butyl phenyl substituent with respect to the mean plane defined by the porphyrin ring are 44.8(1)° and 87.1(1)°. The plane passing through the cyclopentadienyl ring of the cobalt sandwich compound makes an angle of 42.5(2)° with the phenyl unit attached *trans* to it. Similar to the A-type porphyrin 3, the *trans*-AB type porphyrin 4 also shows only a small in-

plane distortion, and the core size elongation parameter was found to be 0.080 Å.

To observe the effect of size of central metal ion on the type and extent of distortion of metal sandwich derived AB type porphyrin molecules, we have determined crystal structures of the Pd and Ni coordinated porphyrins, as well as the free base porphyrin keeping the same bulky substituents in the *trans*-AB porphyrin unit (compounds 5, 7, and 9). Interesting variations in the extent of in-plane and out-of-plane distortions of porphyrin macrocycles were observed.

Interestingly molecular structures of the *trans*-AB porphyrins 5, 7, and 9 showed *syn* orientation with respect to the porphyrin macrocycle of both of the metal sandwich units in spite of the sterically bulky nature of the cobalt sandwich substituent (Figure 5). The reported structure of the analogous *trans*-AB type 5,15-diferrocenyl-2,8,12,18-tetraethyl-3,7,13,17-tetramethylporphyrin³⁶ also showed *syn* orientation for both the ferrocene units. The mean plane passing through the porphyrin macrocycle makes angles of 41.9(1) and 46.3(1)° for 7, 43.5(2) and 39.9(2)° for 5, and 45.0(3) and 45.2(3) for 9

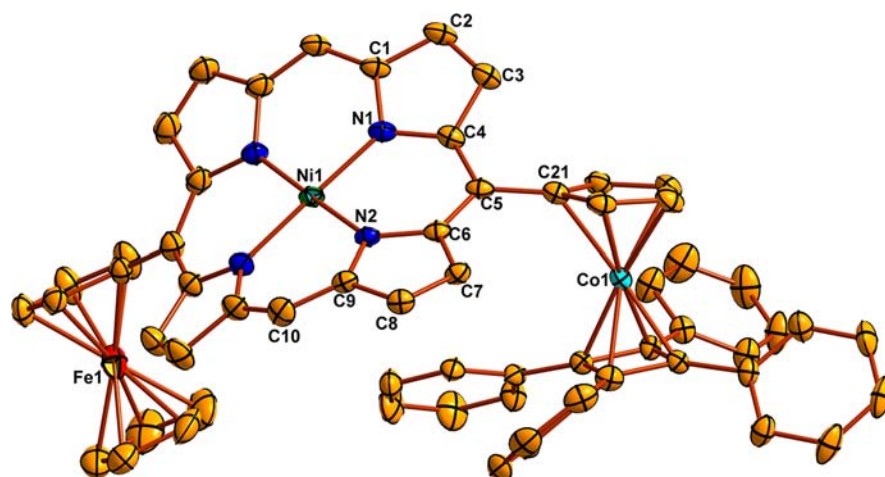


Figure 6. Molecular structure of the *trans*-AB-type porphyrin **7**. Thermal ellipsoids are drawn at the 30% probability level. All hydrogen atoms are omitted for clarity. Selected bond lengths (Å) and angles (deg) with esd's in parentheses C(1)–C(2) 1.429(6); C(2)–C(3) 1.334(6); C(3)–C(4) 1.445(5); C(4)–C(5) 1.400(5); Ni(1)–N(1) 1.909(3); C(4)–C(5)–C(6) 120.0(4); C(11)–C(10)–C(9) 124.3(4).

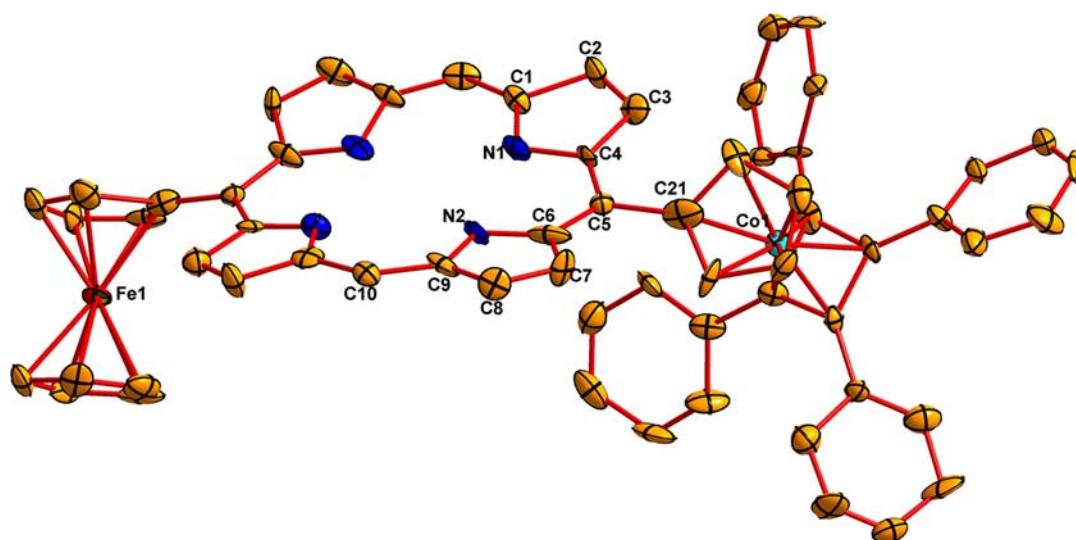


Figure 7. Molecular structure of the *trans*-AB-type demetalated porphyrin **9**. Thermal ellipsoids are drawn at the 30% probability level. All hydrogen atoms are omitted for clarity. Selected bond lengths (Å) and angles (deg) with esd's in parentheses C(1)–C(2) 1.528(12); C(2)–C(3) 1.308(13); C(3)–C(4) 1.452(11); C(7)–C(8)–C(9) 107.6(8); C(3)–C(2)–C(1) 107.6(9); C(2)–C(3)–C(4) 108.7(9).

with the cyclopentadienyl rings of the ferrocene and η^5 -CpCo(η^4 -C₄Ph₄) units, respectively. For compound **7**, the porphyrin bound cyclopentadienyl rings of ferrocene and η^5 -CpCo(η^4 -C₄Ph₄) make an angle of 25.4(2)° with each other, while the corresponding angles in the case of compounds **5** and **9** were found to be 83.0(3)° and 89.9(4)° respectively (Figure 5–7).

The two bulky substituents, ferrocene and η^5 -CpCo(η^4 -C₄Ph₄), at the *meso* positions of the *trans*-AB-porphyrins **5**, **7**, and **9** have been found to induce a ruffle type distortion in the porphyrin skeleton. While replacing the Pd(II) ion of **5** by a smaller Ni(II) ion (**7**), an increase in the magnitude of the ruffle type distortion was observed (Figure 10B). The tilt angles of the individual pyrrole rings with respect to the mean plane passing through the porphyrin ring were found to be 9.1(3), 9.3(3), 8.3(3), and 9.6(3)° in the case of **9**, 10.5(2), 11.2(2), 10.1(2), and 12.6(2)° in the case of **5**, 20.1(1), 19.8(1), 21.5(1), and 20.8(1)° in the case of **7**. This clearly shows that highest out-of-plane tilt of the pyrrole unit with respect to mean plane defined by the porphyrin ring is observed in the case of **7**.

For the free base porphyrin **9**, it was found that the bulky cobalt sandwich unit induces significant strain (Figure 7). The in-plane distortion was found to be maximum (0.38 Å) in the case of the free base porphyrin **9** compared to 0.11 Å of **5** and 0.06 Å in the case of **7**. The Ni(II) coordinated *trans*-AB porphyrin **7** shows the maximum out-of-plane distortion, possibly due to the smaller size of nickel and shorter Ni–N bond distances which were found to be in the range of 1.903(4)–1.914(4) Å. The displacement of each atom from the mean plane defined by the porphyrin ring has been found to vary in the range of –0.629 to 0.698 Å in the case of **7**, –0.400 to 0.331 Å in **5**, and –0.330 to 0.381 Å in the case of **9** (Figure 10, panels D, C, and E, respectively). A similar type of ruffling has also been reported in the case of Ni(II) coordinated porphyrin 5,10,15,20-tetrabutyl-2,3,7,8,12,13,17,18-octaethylporphyrinatonicel(II).³⁴

The crystal structure of compound **11** indicated that the molecule has a center of symmetry, and both the cobalt sandwich units are in *anti* orientation with respect to the porphyrin macrocycle (Figure 8). This is in contrast to the

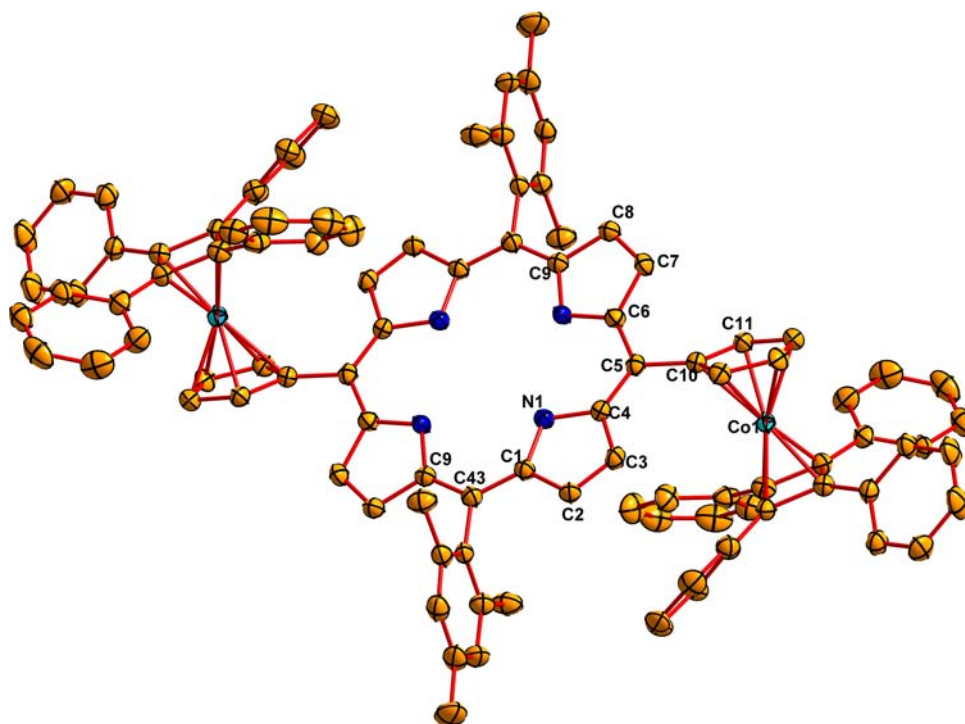


Figure 8. Molecular structure of *trans*-A₂B₂-type porphyrin **11**. Thermal ellipsoids are drawn at the 30% probability level. All hydrogen atoms are omitted for clarity. Selected bond lengths (Å) and angles (deg) with esd's in parentheses C(1)–C(2) 1.425(9); C(2)–C(3) 1.328(9); C(3)–C(4) 1.434(9); C(4)–C(5) 1.393(9); N(1)–C(1) 1.381(7); C(6)–C(5)–C(4) 122.7(4); C(11)–C(10)–C(5) 124.3(3); C(1)–C(43)–C(9) 126.9(4).

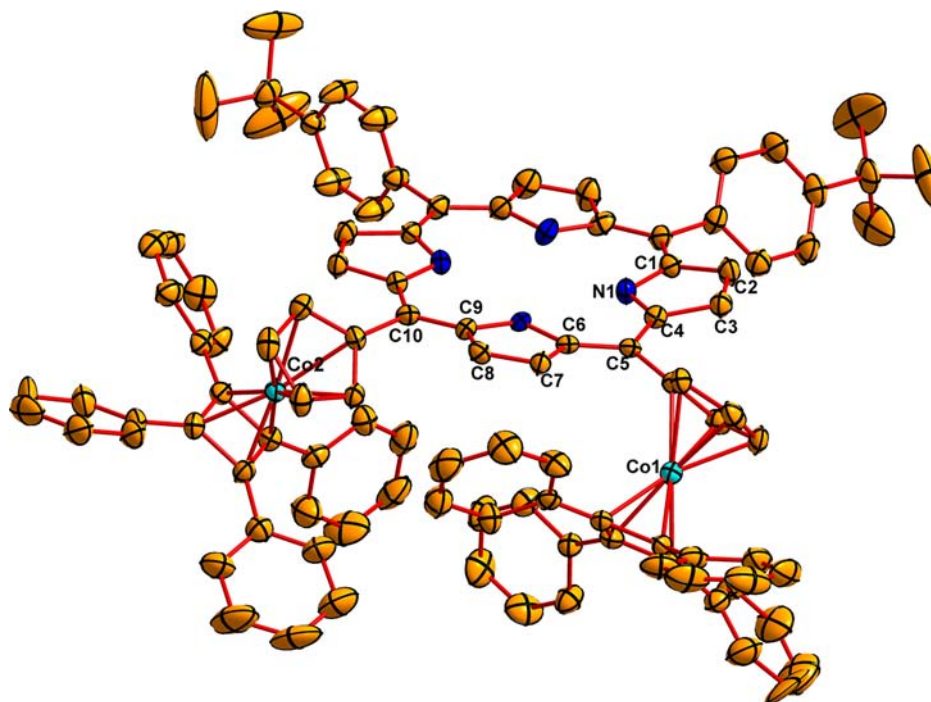


Figure 9. Molecular structure of *cis*-A₂B₂-type porphyrin **13**. Thermal ellipsoids are drawn at the 30% probability level. All hydrogen atoms are omitted for clarity. Selected bond lengths (Å) and angles (deg) with esd's in parentheses C(1)–C(2) 1.431(9); C(2)–C(3) 1.332(8); C(3)–C(4) 1.451(8); C(4)–C(5) 1.396(7); N(1)–C(1) 1.362(7); C(4)–C(5)–C(6) 124.0(6); C(3)–C(2)–C(1) 108.0(6); C(2)–C(3)–C(4) 106.2(6); C(4)–C(5)–C(6) 124.2(6).

theoretical studies reported for the analogous ferrocene containing porphyrin 5,15-bisferrocenyl-10,20-diphenyl porphyrin^{4b} where based on DFT calculations both the ferrocene units were predicted to be in *syn* orientation. The macrocycle of **11** shows only a significant in-plane distortion, and the core

elongation parameter was found to be 0.251 Å. The plane passing through all the 24 atom of porphyrin macrocycle in **11** makes an angle of 42.5(1)° with the cyclopentadienyl rings of both of the cobalt sandwich substituents. The dihedral angle

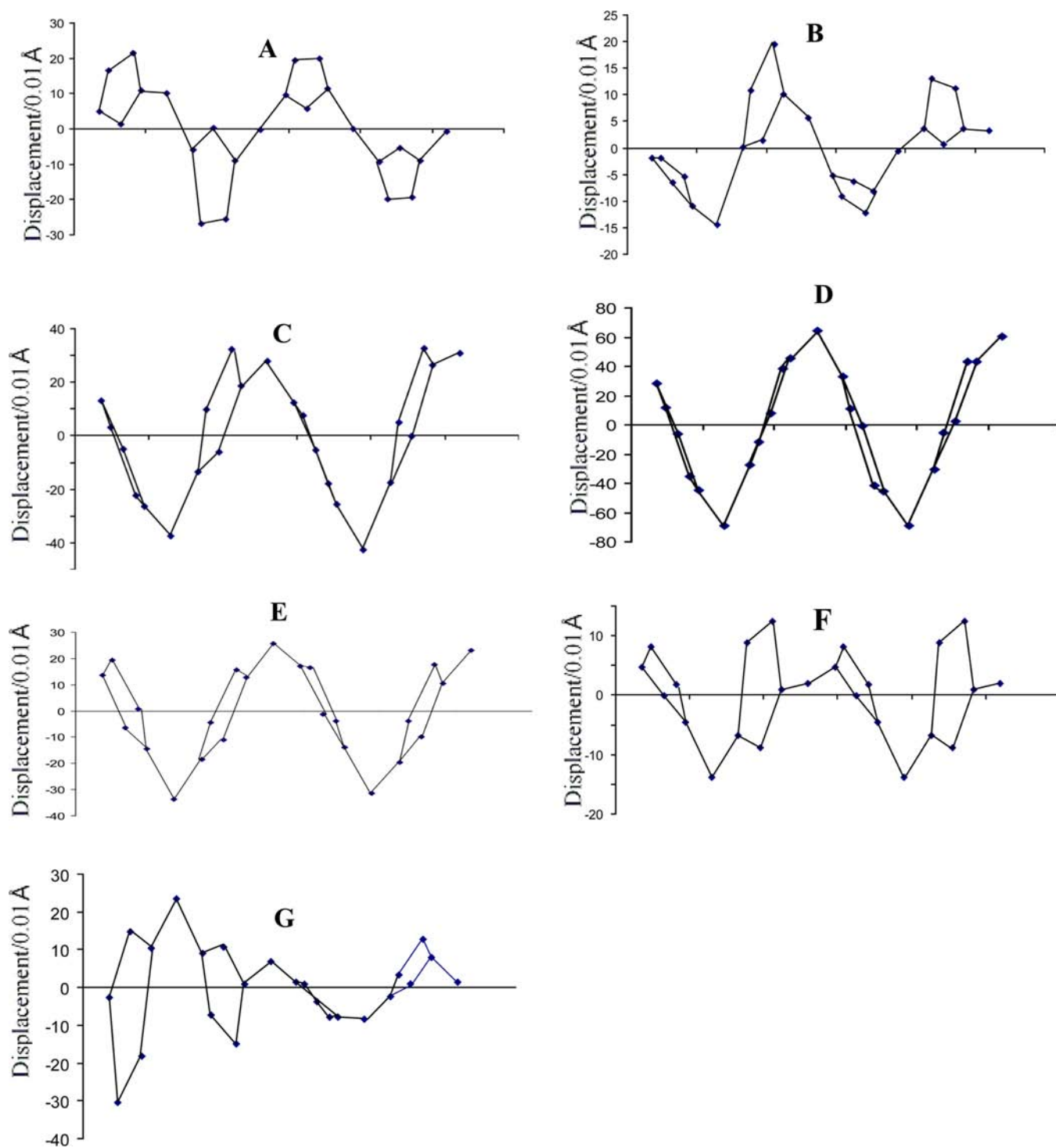


Figure 10. Diagram showing the out-of-plane displacements (in unit of 0.01 Å) of the porphyrin core atoms of (A) 3, (B) 4, (C) 5, (D) 7, (E) 9, (F) 11, (G) 13 from the mean plane of the $C_{20}N_4$ porphyrin core.

between the phenyl rings and the porphyrin macrocycle was found to be $87.8(1)^\circ$.

The structure of compound 13 illustrates that the molecule has interestingly both the cobalt sandwich units in *syn* orientation with respect to the porphyrin macrocycle despite having two sterically hindered tetraphenylcyclobutadiene units in close proximity (Figure 9). This observation is also in contrast to the analogous ferrocene containing porphyrin, 5,10-biferrocenyl-15,20-diphenyl porphyrin whose structure has been predicted to have the ferrocene units in *anti* orientation

based on DFT calculations.^{4b} The displacement of each atom from the mean plane defined by all the 24 porphyrin ring atoms has been found to vary in the range of -0.210 to 0.331 Å in the case of 13 (Figure 10G). The plane passing through the mean plane of the porphyrin macrocycle in 13 makes an angle of $41.9(2)$ and $45.8(2)^\circ$ with the cyclopentadienyl rings of both of the cobalt sandwich units. The two cyclopentadienyl rings of the cobalt sandwich units makes an angle of the $58.7(4)^\circ$ with respect to each other. In contrast to the structure of the *trans*- A_2B_2 porphyrin 11, which shows significant in-plane distortion,

the macrocycle in *cis*-A₂B₂ type porphyrin **13** shows only a small in-plane distortion, and the core elongation parameter was found to be 0.085 Å.

Electrochemical Studies. The electrochemical behavior of cobalt sandwich based porphyrins **3–13** was investigated by cyclic voltammetric analysis using tetra-butylammonium hexafluorophosphate as the supporting electrolyte in dichloromethane. In general, porphyrins show two oxidation and two reduction waves corresponding to the formation of mono- and dication as well as mono- and dianion of the porphyrin ring.³⁷ In the porphyrin-cobalt sandwich conjugates, additional redox couple corresponding to the oxidation of cobalt sandwich unit can also be expected.

The cobalt sandwich derived porphyrins **3–13** show two ring-centered one-electron transfer reduction waves, each corresponding to single electron reduction, observed in the range of –1.09 to –1.21 V and –1.22 to –1.84 V, respectively. These values are close to –1.29 and –1.67 V observed in the case of H₂TTPFc ferrocene conjugates of *meso*-5,10,15,20-*terta*(*p*-tolyl) porphyrin.³

Table 1. Cyclic Voltammetric Data for Cobalt Sandwich-Containing Porphyrins in a DCM/TBAP System

compound	Ox ₃ (P)	Ox ₂ (Cb)	Ox ₁ (Fc)	R ₁ (P)	R ₂ (P)
3	1.50	0.87		–1.20	–1.80
4	1.26	0.82		–1.02	–1.43
5	1.23	0.82	0.47	–1.10	–1.60
6	1.40	0.90		–1.15	–1.47
7	1.25	0.92	0.52	–1.16	–1.53
8	1.26	0.83	0.44	–1.20	–1.82
9	1.27	0.92	0.52	–1.09	–1.84
10	1.29	0.85		–1.05	–1.63
11	1.10	0.81		–1.12	–1.45
12	1.20	0.93		–1.10	–1.22
13	1.16	0.80		–1.21	–1.73

All potentials are referenced to the Ag/AgCl. Potential of the working glassy electrode was varied in the range of –2.0 to +1.5 V. P = porphyrin-centered process, Cb = cobalt sandwich centered process, Fc = ferrocene-centered process, Ox = oxidation, R = reduction. All reductions are porphyrin core centered.

The A-type porphyrin **3** having a CpCoC₄Ph₄ unit at one of its *meso* positions showed a single electron oxidation of the cobalt sandwich substituent Co(I/II) at 0.87 V (100 mV scan rate) which is close to the reported value of 0.92 V for the cobalt sandwich substituted stilbene derivative, [Co(η^4 -C₄Ph₄)- η^5 -C₅H₄CH=CHC₆H₅)]³⁸. This peak was assigned as quasi reversible as the peak current ratio $i_{\text{rev}}/i_{\text{fwd}}$ was 0.33. One irreversible peak at +1.50 V was also observed which is possibly due to a porphyrin ring centered oxidation. The reported second oxidation of the cobalt sandwich substituent [Co(II)/(III)] occurs at more than 1.50 V under similar measurement conditions, and therefore there is less probability for this peak to be due to the cobalt center. Compound **3** also showed the two ring-centered one-electron transfer reduction waves at –1.20 and –1.80 V for the formation of monoanion and dianion respectively of the porphyrin ring.

In contrast to compounds **3** and **4** which showed quasi reversible peaks at 0.87 and 0.82 V for the cobalt sandwich substituent, corresponding signal for compounds **5–13** showed an irreversible peak in the range of 0.81–0.93 V. This is

consistent with the reported result for the 9-anthracenyl stilbene derived cobalt sandwich [Co(η^4 -C₄Ph₄)- η^5 -C₅H₄CH=CHC₁₄H₉)]³⁸ which showed an irreversible peak at 0.89 V. In addition to the peak at 0.87 V, *trans*-AB porphyrin **4** also showed a second wave at 1.28 V, which is possibly due to the oxidation of the porphyrin core. In contrast to compound **4**, compound **6** showed two oxidation peaks at a comparatively higher potential at 0.91 and 1.40 V possibly due to the presence of the electronegative pentafluorobenzene as one of the *meso* substituents.

The *trans*-AB type porphyrins **5**, **7**, **8**, and **9**, all having ferrocene as one of the *meso* substituent exhibited a one-electron reversible oxidation in the range of +0.47 to +0.52 V due to ferrocene which is close to the 0.41 V observed in the case of bis-1,1'-(porphyrinyl)ferrocene.³⁹ These peaks were assigned as reversible as the peak current ratio $i_{\text{pa}}/i_{\text{pc}}$ was close to unity (see Supporting Information). Irreversible waves at 0.82, 0.92, 0.83, and 0.92 V were observed for *trans*-AB type porphyrins **5**, **7**, **8**, and **9**, respectively, which were assigned as cobalt sandwich centered oxidation process.³⁸ For *trans*-AB porphyrins **5**, **7**, **8**, and **9**, an irreversible wave was observed in the range of 1.23–1.27 V due to the porphyrin centered oxidation. Interestingly compound **5**, **7**, **9** showed the ferrocene³⁹ and a cobalt center based oxidation³⁸ close to the reported value indicates that there is no significant electro communication between these redox centers, which can also be evident by its crystal structure which shows that porphyrin macrocycles are not in-plane to that of the ferrocene and cobalt sandwich moiety (see Supporting Information).

A similar porphyrin based irreversible oxidation at 1.27 V was reported for the bis-1,1'-(porphyrinyl) ferrocene.³⁹ The free base *trans*-AB porphyrin **9** showed the ferrocene based oxidation at 0.52 V. In addition to this, it also showed two other irreversible oxidation waves, one at 0.92 due to the cobalt sandwich unit and the other at 1.27 V due to the porphyrin ring oxidation. The two porphyrin ring centered reduction peaks for **9** were observed at –1.09 and –1.84 V.

The *trans*-A₂B₂ porphyrin **10** showed three closely separated peaks at 0.85, 1.14, and +1.29 V. The first two peaks are due to the oxidation of the cobalt sandwich units. The third irreversible oxidation which was observed at +1.27 V is possibly due to the oxidation of the porphyrin core (see Supporting Information). This is close to the 1.16 V reported in the case of the analogous *trans*-A₂B₂ type 5,15-bisferrocenyl-10,20-bis-(pentafluorophenyl) porphyrin.³

Compared to **10**, the *trans*-A₂B₂ porphyrin **11** showed separate oxidation peaks at 0.81, 1.10, and 1.38 V. Apart from these three oxidation peaks, it also showed the expected reduction waves at –1.12 and –1.45 V of the porphyrin ring. Similar to the *trans*-A₂B₂ porphyrin **11**, the *cis*-A₂B₂ porphyrin **13** showed three different oxidation peaks at 0.81, 1.15, and 1.29 V. However, in contrast to the *cis*-A₂B₂ porphyrin **13** (reduction peaks at –1.21, –1.73 V) the AB₃ porphyrin **12** showed two reduction waves at –1.10 and 1.22 V indicating the relative ease of reduction of this compound (see Supporting Information).

CONCLUSIONS

The synthesis and structural characterization of the first examples of porphyrins substituted at the *meso* positions with sterically hindered η^5 -CpCo(η^4 -C₄Ph₄) cobalt sandwich units are described. The synthesis of these compounds are made possible by the facile preparation of the first dipyrromethane

Table 2. X-ray Crystal Structure Parameters of Compounds 1–5, 7, 9, 11, and 13

parameters	1	2	3	4	5	7	9	11	13
formula	C ₄₂ H ₃₃ CoN ₂	C ₄₆ H ₃₅ Cl ₆ CoN ₂ O ₂ · 2CHCl ₃	C ₃₃ H ₃₅ CoN ₄ Pd	C ₆₃ H ₄₇ CoN ₄ Pd· C ₇ H ₈	C ₆₃ H ₄₃ CoFeN ₄ Pd	C ₆₃ H ₄₃ CoFeN ₄ Ni	C ₆₃ H ₄₅ CoFeN ₄	C ₁₀₄ H ₈₀ Co ₂ N ₄ · 4CHCl ₃	C ₁₀₆ H ₈₄ Co ₂ N ₄
MW	624.63	919.39	893.18	1117.51	1077.2	1029.48	972.81	1981.05	1531.64
cryst syst	monoclinic	triclinic	triclinic	triclinic	triclinic	triclinic	triclinic	triclinic	triclinic
space group	<i>P</i> 2 ₁ / <i>n</i>	<i>P</i> $\bar{1}$	<i>P</i> $\bar{1}$	<i>P</i> $\bar{1}$	<i>P</i> $\bar{1}$	<i>P</i> $\bar{1}$	<i>P</i> $\bar{1}$	<i>P</i> $\bar{1}$	<i>P</i> $\bar{1}$
<i>a</i> (Å)	11.031(2)	12.508(2)	9.476(2)	11.446(4)	10.122(2)	10.511(3)	11.483(5)	11.844(2)	16.515(9)
<i>b</i> (Å)	31.737(4)	14.058(2)	12.502(2)	15.242(5)	13.993(3)	14.630(4)	12.921(5)	15.170(2)	16.806(9)
<i>c</i> (Å)	18.458(3)	14.392(2)	16.647(3)	15.716(5)	21.215(4)	16.892(4)	19.322(8)	15.832(3)	18.558(10)
α (deg)	90	86.351(3)	78.860(4)	98.590(7)	102.319(4)	80.597(4)	79.541(10)	112.919(3)	84.940(11)
β (deg)	104.216(3)	66.987(2)	80.649(4)	90.968(7)	99.692(4)	84.627(4)	89.485(11)	107.210(3)	66.155(11)
γ (deg)	90	67.107(2)	79.720(4)	97.920(7)	105.398(4)	78.583(5)	76.647(10)	97.881(3)	67.822(10)
<i>V</i> (Å ³)	6264.2(2)	2134.1(5)	1887.1(6)	2683.2(2)	2748.5(10)	2506.9(11)	2741.4(19)	2397.6(7)	4350(4)
<i>Z</i>	8	2	2	2	2	2	2	1	2
λ (Å)	0.71073	0.71073	0.71073	0.71073	0.71073	0.71073	0.71073	0.71073	0.71073
ρ_{calc} (g/cm ³)	1.325	1.431	1.572	1.383	1.302	1.364	1.468	1.372	1.169
μ (mm ⁻¹)	0.581	0.818	0.962	0.692	0.923	1.029	0.906	0.731	0.431
goodness of fit	1.254	1.083	1.154	1.089	0.949	1.023	1.069	1.023	0.843
θ range	1.31–25.0	1.55–25.00	1.26–25.00	1.74–25.00	1.57–25.0	1.44–25.00	1.65–25.00	1.51–25.0	1.31–25.00
total reflections	59736	20553	18067	14772	14251	13136	13474	12655	22885
unique reflections	11012	7513	6602	9448	9668	8842	9506	8433	15323
observed data [<i>I</i> > 2 σ (<i>I</i>)]	9665	6314	5370	7041	7019	6741	4147	6110	5974
<i>R</i> _{int}	0.0616	0.03	0.0684	0.0414	0.0277	0.0247	0.0873	0.0317	0.0674
<i>R</i> ₁ , <i>wR</i> ₂ [(<i>I</i> > 2 σ (<i>I</i>)] ^a	0.0818, 0.1669	0.0782, 0.2041	0.0629, 0.1290	0.0684, 0.1519	0.0486, 0.1287	0.0563, 0.1484	0.1170, 0.2766	0.0838, 0.2309	0.0799, 0.1858
<i>R</i> ₁ , <i>wR</i> ₂ (all data) ^a	0.0954, 0.1735	0.0903, 0.2138	0.0826, 0.1364	0.0955, 0.1671	0.0643, 0.1405	0.0709, 0.1583	0.2034, 0.3193	0.1072, 0.2554	0.1728, 0.2241

$$^a R_1 = \frac{\sum |F_o| - |F_c|}{\sum |F_o|}; wR_2 = \frac{\sum (|F_o|^2 - |F_c|^2)^2}{\sum |F_o|^2}$$

derivative of $(\eta^5\text{-Cp})\text{Co}(\eta^4\text{-C}_4\text{Ph}_4)$ and its 1,9-diformyl derivative. A set of highly air and moisture stable porphyrins of the type A, *trans*-A₂B₂, *cis*-A₂B₂, and A₃B where A is $\eta^5\text{-CpCo}(\eta^4\text{-C}_4\text{Ph}_4)$ have been prepared with the sandwich unit occupying the *meso* positions. For the first time, rational methods have been adopted to introduce two different organometallic fragments such as ferrocene and $(\eta^5\text{-Cp})\text{Co}(\eta^4\text{-C}_4\text{Ph}_4)$ on a porphyrin periphery, which resulted in better selectivity. A rational method involving metal template was also employed for the first time for the synthesis of novel A- and *trans*-A₂B type of porphyrins. While base-catalyzed reactions of dipyrromethane with its diformyl derivative did not yield isolable quantities of $(\eta^5\text{-Cp})\text{Co}(\eta^4\text{-C}_4\text{Ph}_4)$ *meso*-disubstituted porphyrins, an acid-catalyzed reaction of the aldehyde $\eta^5\text{-}[\text{C}_5\text{H}_4(\text{CHO})]\text{Co}(\eta^4\text{-C}_4\text{Ph}_4)$ with sterically hindered dipyrromethanes gave selectively *trans*-A₂B₂ type porphyrins. In contrast, reactions of the aldehyde with a sterically unhindered dipyrromethane under the same conditions gave *cis*-A₂B₂ and A₃B type porphyrins, the latter resulting from scrambling. These novel examples of *cis* and *trans* $(\eta^5\text{-Cp})\text{Co}(\eta^4\text{-C}_4\text{Ph}_4)$ disubstituted porphyrins were also structurally characterized. The structures of these compounds show interesting differences in the spatial orientation of the sandwich units when compared with the theoretically predicated structures of analogous ferrocene derivatives. The number and position of $(\eta^5\text{-Cp})\text{Co}(\eta^4\text{-C}_4\text{Ph}_4)$ units as well as size of metal ions have been found to affect the extent of planarity of the porphyrin rings. The number of $(\eta^5\text{-Cp})\text{Co}(\eta^4\text{-C}_4\text{Ph}_4)$ units at the *meso* positions of a porphyrin also seem to have a significant effect on the bathochromic shift on the Soret band of the porphyrin ring compared to porphyrins having ferrocene at the *meso* positions.

EXPERIMENTAL SECTION

General Methods. All manipulations of the complexes were carried out using standard Schlenk techniques under nitrogen atmosphere. All the solvents were freshly distilled using standard procedures. The compounds ferrocenecarbaldehyde, 4-*tert*-butylbenzaldehyde, pentafluorobenzaldehyde, mesitaldehyde, DDQ, triethylamine, *n*-propylamine, $\text{PdCl}_2(\text{PhCN})_2$, $\text{Ni}(\text{acac})_2$ and zinc acetate were procured from Aldrich and were used as such. Pyrrole was distilled from calcium hydride under nitrogen atmosphere before use. Sodium salt of carbomethoxycyclopentadiene,⁴⁰ tris-(triphenylphosphine)cobalt chloride,⁴¹ $(\eta^5\text{-formyl cyclopentadienyl})\text{-}(\eta^4\text{-tetraphenylcyclobutadiene})\text{cobalt}$,^{15b} ferrocenyl dipyrromethane,²⁰ *meso*-4-*tert*-butylphenyldipyrromethane,⁴² *meso*-mesityldipyrromethane,⁴³ and *meso*-pentafluorophenyldipyrromethane³⁰ were prepared according to literature procedures.

Instrumentation. ¹H and ¹³C{¹H} spectra were recorded on a Bruker Spectrospin DPX-300 NMR spectrometer at 300 and 75.47 MHz, respectively. Elemental analyses were carried out on a Carlo Erba CHNSO 1108 elemental analyzer. Mass spectra were recorded on Bruker Micro-TOF QII quadrupole time-of-flight (Q-TOF) mass spectrometer. Electronic spectra were recorded by using Perkin-Elmer Bio Lambda 20 UV/vis spectrophotometer. Cyclic voltammetric measurements were performed on a (Autolab PGSTAT302N) electrochemical analyzer. A glassy carbon working electrode, a platinum wire auxiliary electrode and Ag/AgCl reference electrode were used in a standard three-electrode configuration. The ferrocene/ferrocenium couple occurs at $E_{1/2} = +0.38$ V versus Ag/AgCl under the same experimental conditions.

X-ray Crystallography. Suitable crystals of compounds 1, 2, 3, 4, 5, 7, 9, 11, and 13 were obtained by slow evaporation of their saturated solutions in ethyl acetate/hexane, dichloromethane/toluene or chloroform/toluene solvent mixtures. Single-crystal diffraction studies were carried out on a Bruker SMART APEX CCD diffractometer with a Mo $K\alpha$ ($\lambda = 0.71073$ Å) sealed tube. All crystal structures were

solved by direct methods. The program SAINT (version 6.22) was used for integration of the intensity of reflections and scaling.^{44a} The program SADABS was used for absorption correction.^{44b} The crystal structures were solved and refined using the SHELXTL (version 6.12) package.^{44c} All hydrogen atoms were included in idealized positions, and a riding model was used. Non-hydrogen atoms were refined with anisotropic displacement parameters. Table 2 lists the data collection and structure solving parameters for compounds 1–5, 7, 9, 11, and 13. The data for all structures were collected at room temperature. The highly distorted solvent molecules in the crystals of complexes 4, 7, and 13 were omitted using the SQUEEZE algorithm. The resulting new data set after this omission was generated, and the structure was refined to convergence. Selected bond distances and angles for all compounds are given in the Supporting Information.

Synthesis of $\eta^5\text{-}[(\text{C}_4\text{H}_4\text{N})_2\text{CHC}_5\text{H}_4]\text{Co}(\eta^4\text{-C}_4\text{Ph}_4)$ 1. A mixture of pyrrole (3.11 mL, 43.00 mmol) and $\eta^5\text{-}[\text{C}_5\text{H}_4(\text{CHO})]\text{Co}(\eta^4\text{-C}_4\text{Ph}_4)$ (0.57 g, 1.10 mmol) was degassed by bubbling argon for 10 min. Trifluoroacetic acid (0.02 mL, 0.11 mmol) was added, and the mixture was stirred for 2 h at room temperature, diluted with CH_2Cl_2 , and washed with 0.1 M NaOH, followed by water. The organic layer was dried over anhydrous sodium sulfate and concentrated under reduced pressure, and the unreacted pyrrole was removed by vacuum distillation at room temperature. The resulting dark yellow viscous semisolid was chromatographed through neutral alumina using 10% ethyl acetate/hexane as eluent to give a yellow crystalline solid which was identified as $\eta^5\text{-}[(\text{C}_4\text{H}_4\text{N})_2\text{CHC}_5\text{H}_4]\text{Co}(\eta^4\text{-C}_4\text{Ph}_4)$ (1). Yield 0.63 g, 87% Mp: 210–212 °C (dec.). Anal. Calcd. for $\text{C}_{42}\text{H}_{33}\text{CoN}_2$: C, 80.76; H, 5.32; N, 4.48. Found: C, 80.78; H, 5.29; N, 4.52. ¹H NMR (δ , 300 MHz, CDCl_3): 4.56 (4H, s, Cp), 4.69 (1H, s), 5.68 (2H, s), 6.05 (2H, s), 6.44 (2H, s) 7.23–7.30 (20H, m, Ph). ¹³C NMR: 77.04 (C_4Ph_4), 82.58, 82.79, 100.97 (CpC), 106.38, 108.03, 116.36, 126.26 ($\text{C}_4\text{H}_4\text{N}$), 128.00, 128.13, 128.83, 132.41 (PhC), 136.04 (CH– $\text{C}_4\text{H}_4\text{N}$); HRMS: Calcd. for $\text{C}_{42}\text{H}_{34}\text{CoN}_2$: 625.2054, Found: 625.2018.

Synthesis of *meso*- $\{\eta^5\text{-}[(\text{CHO})(\text{C}_4\text{H}_3\text{N})_2\text{CHC}_5\text{H}_4]\text{Co}(\eta^4\text{-C}_4\text{Ph}_4)\}$ 2. The dipyrromethane 1 (0.62 g, 1.00 mmol) was dissolved in 3.0 mL of dimethyl formamide cooled to 0 °C and stirred for 20 min. In another flask, Vilsmeier reagent was prepared by adding POCl_3 (1.5 mL, 16.00 mmol) dropwise to dimethylformamide (10.00 mL) at 0 °C. To the cold solution of dipyrromethane 1 Vilsmeier reagent (0.80 mL, 2.1 equiv) was added dropwise, and the mixture was stirred at 0 °C for 2 h. The reaction was quenched by adding a saturated aqueous sodium acetate solution, and the solution was extracted with ethyl acetate. The organic phase were washed first with brine and then with water. It was then dried over anhydrous sodium sulfate. Afterward, all solvents were evaporated off, and the crude product was chromatographed through neutral alumina using an ethyl acetate/hexane 20% mixture as the eluent. The compound obtained as orange red crystals after slow evaporation was characterized as *meso*- $\{\eta^5\text{-}[(\text{CHO})(\text{C}_4\text{H}_3\text{N})_2\text{CHC}_5\text{H}_4]\text{Co}(\eta^4\text{-C}_4\text{Ph}_4)\}$ 2. Yield: 0.29 g, 65%. Mp: 232–234 °C (dec.) Anal. Calcd. for $\text{C}_{46}\text{H}_{35}\text{Cl}_6\text{CoN}_2\text{O}_2$: C, 60.09; H, 3.84; N, 3.05. Found: C, 60.11; H, 3.80; N, 3.12. ¹H NMR (δ , 300 MHz, CDCl_3): 4.50 (2H, s, Cp), 4.56 (2H, s, Cp), 4.80 (1H, s), 5.76 (2H, d, ³J = 2.0 Hz), 6.80 (2H, d, ³J = 2.1 Hz), 7.18–7.30 (20H, m, Ph), 9.33 (2H, s, NH), 10.44 (2H, s, CHO). ¹³C NMR: 75.03 (C_4Ph_4), 82.86, 83.40, 96.60 (CpC), 110.63, 122.27, 125.28, 126.44 ($\text{C}_4\text{H}_4\text{N}$), 128.21, 128.76, 129.02, 132.58 (PhC), 141.32 [CH–($\text{C}_4\text{H}_4\text{N}$)₂], 179.01 (–CHO) HRMS: Calcd. for $\text{C}_{44}\text{H}_{33}\text{CoN}_2\text{O}_2\text{Na}$: 703.1772, Found: 703.1766.

Synthesis of the A-Type Porphyrin 3. A mixture of 1,9-diformyldipyrromethane 2 (0.68 g, 1.0 mmol), dipyrromethane (0.14 g, 1.00 mmol), KOH (0.28 g, 5.00 mmol), and $\text{Pd}(\text{C}_6\text{H}_5\text{CN})_2\text{Cl}_2$ (0.23 g, 0.60 mmol) in EtOH was heated at reflux in the open for 1 h. Afterward the solvent was removed under a vacuum, and chromatography of the crude product using ethyl acetate/hexane 5% mixture afforded the A type porphyrin 3. Yield: 0.16 g, 18%. Mp: 225–227 °C (dec.). Anal. Calcd. for $\text{C}_{53}\text{H}_{35}\text{CoN}_4\text{Pd}$: C, 71.27; H, 3.95; N, 6.27. Found: C, 71.30; H, 3.89; N, 6.34. ¹H NMR (δ , 300 MHz, CDCl_3): 5.23 (2H, s, Cp), 5.83 (2H, s, Cp), 6.69–7.11 (20H, m, Ph), 8.75 (2H, d, ³J = 5.1 Hz), 9.23 (4H, m), 9.73 (2H, d, ³J = 4.8 Hz),

10.00 (2H, s), 10.13 (1H, s). UV/vis (CH₂Cl₂; λ_{max} nm 400 (4.39), 531 (3.77), 575 (3.47).

General Procedure for Synthesis of Palladium(II) *trans*-AB-Porphyrins 4–6. A mixture of 1,9-diformyldipyrromethane **2** (1 equiv), *meso* aryl- and ferrocenyl-substituted dipyrromethane (1 equiv), KOH (5 equiv), and Pd(C₆H₅CN)₂Cl₂ (0.6 equiv) in EtOH was heated at reflux under open conditions for 1 h. Afterward the solvent was removed under a vacuum, and chromatography of the crude product using ethyl acetate and hexane (3–5%) afforded the *trans*-AB type palladium coordinated porphyrin.

Synthesis of Porphyrin 4. The reaction was performed following the general procedure using **2** (0.14 g, 0.20 mmol), *meso*-4-*tert*-butylphenyldipyrromethane (0.05 g, 0.20 mmol), KOH (0.06 g, 1.00 mmol), and Pd(C₆H₅CN)₂Cl₂ (0.05 g, 0.12 mmol). Compound **4** was obtained as a red colored solid. Yield: 0.03g, 14%. Mp: 242–244 °C (dec.). Anal. Calcd. for C₇₀H₅₅CoN₄Pd: C, 75.23; H, 4.96; N, 5.01. Found: C, 75.21; H, 4.87; N, 5.16. ¹H NMR (δ , 300 MHz, CDCl₃): 1.63 (9H, s, CH₃), 5.29 (2H, s, Cp), 5.90 (2H, s, Cp), 6.71–7.31 (20H, m, PhH), 7.78 (2H, d, ³J = 8.4 Hz), 8.14 (2H, d, ³J = 8.1 Hz), 8.79 (2H, d, ³J = 4.8 Hz), 8.99 (2H, d, ³J = 4.5 Hz), 9.18 (2H, d, ³J = 4.8 Hz), 9.76 (2H, d, ³J = 4.8 Hz), 10.02 (2H, s). UV/vis (CH₂Cl₂); λ_{max} nm (log ϵ , M⁻¹ cm⁻¹) 411 (4.45), 526 (4.23), 563 (4.12).

Synthesis of Porphyrin 5. The reaction was performed following the general procedure using **2** (0.10 g, 0.14 mmol), *meso*-ferrocenyl dipyrromethane (0.05 g, 0.14 mmol), KOH (0.04 g, 0.73 mmol), and Pd(C₆H₅CN)₂Cl₂ (0.03 g, 0.09 mmol). Compound **5** was obtained as a green-colored solid. Yield: 0.038 g, 24%. Mp: 188–190 °C (dec.). Anal. Calcd. for C₇₀H₅₁CoFeN₄Pd: C, 71.90; H, 4.40; N, 4.79. Found: C, 71.93; H, 4.51; N, 4.73. ¹H NMR (δ , 300 MHz, CDCl₃): 4.28 (5H, s, Cp), 4.85 (2H, s, Cp), 5.26 (2H, s, Cp_{FC}), 5.50 (2H, s, Cp), 5.85 (2H, d, Cp_{FC}), 6.78–7.70 (20H, m, Ph), 8.71 (2H, d, ³J = 4.8 Hz), 9.15 (2H, d, ³J = 4.8 Hz), 9.64 (2H, d, ³J = 4.8 Hz), 9.89 (2H, s), 10.16 (2H, d, ³J = 4.8 Hz). UV/vis (CH₂Cl₂); λ_{max} nm (log ϵ , M⁻¹ cm⁻¹) 416 (4.58), 538 (4.21), 595 (4.10). MS: Calcd. for C₆₃H₄₃CoN₄Pd: 1076.1204, Found: 1076.7698.

Synthesis of Porphyrin 6. The reaction was performed following the general procedure using **2** (0.14 g, 0.20 mmol), *meso*-pentafluorophenyl dipyrromethane (0.06 g, 0.20 mmol) KOH (0.06 g, 1.00 mmol) and Pd(C₆H₅CN)₂Cl₂ (0.05 g, 0.12 mmol). Compound **6** was obtained as a red-colored solid. Yield: 0.02g, 10% Mp: 235–238 °C (dec.). Anal. Calcd. for C₅₉H₃₄CoF₅N₄Pd: C, 66.90; H, 3.24; N, 5.29. Found: C, 66.82; H, 3.32; N, 5.24. ¹H NMR (δ , 300 MHz, CDCl₃): 5.31 (2H, s, Cp), 5.91 (2H, s, Cp), 7.29–7.32 (20H, m, PhH), 8.79 (2H, d, ³J = 4.8 Hz), 8.90 (2H, d, ³J = 4.5 Hz), 9.26 (2H, d, ³J = 4.8 Hz), 9.77 (2H, d, ³J = 5.1 Hz), 10.06 (2H, s). UV/vis (CH₂Cl₂); λ_{max} nm (log ϵ , M⁻¹ cm⁻¹) 416 (4.77), 528 (4.07), 570 (3.93). MS: Calcd. for C₅₉H₃₄CoF₅ N₄Pd: 1058.1070, Found: 1058.1128.

Synthesis of the Nickel Coordinated Porphyrin 7. 1,9-Diformyl dipyrromethane **2** (0.14 g, 0.20 mmol), 5-ferrocenyldipyrromethane (0.05 g, 0.20 mmol), KOH (0.06 g, 1.00 mmol), and Ni(CH₃COCHCOCH₃)₂ (0.03 g, 0.12 mmol) were placed in a flask fitted with a condenser exposed to air. Ethanol (2.0 mL) was added and the mixture was stirred and heated to reflux for 1 h. The solvent was evaporated, and the residue was chromatographed on neutral alumina to give a dark green-colored solid, which was recrystallized using dichloromethane/hexane mixture to afford crystals which was identified as **7**. Yield: 0.04 g, 17%. Mp: 188–190 °C (dec.). Anal. Calcd. for C₆₄H₄₄Cl₃CoFeN₄Ni: C, 66.91; H, 3.86; N, 4.88. Found: C, 66.96; H, 3.82; N, 4.85. ¹H NMR (δ , 300 MHz, CDCl₃): 3.92 (5H, s, Cp), 4.66 (2H, s, Cp), 5.08 (2H, s, Cp_{FC}), 5.13 (2H, s, Cp), 5.47 (2H, d, Cp_{FC}), 6.54–7.47 (20H, m, Ph), 8.53 (2H, d, ³J = 4.8 Hz), 8.90 (2H, d, ³J = 4.5 Hz), 9.13 (2H, d, ³J = 4.8 Hz), 9.29 (2H, s), 9.65 (2H, d, ³J = 4.8 Hz). UV/vis (CH₂Cl₂); λ_{max} nm (log ϵ , M⁻¹ cm⁻¹) 423 (4.20), 551 (3.87), 608 (3.47). MS: Calcd. for C₆₃H₄₃CoN₄Pd: 1076.1204, Found: 1076.7698.

Synthesis of the Zinc-Coordinated Porphyrin 8. 1,9-Diformyl dipyrromethane **2** (0.14 g, 0.20 mmol) and *n*-propylamine (0.04 mL, 0.50 mmol) in THF (2 mL) were stirred at room temperature for 1 h. After removal of the excess *n*-propylamine and THF under vacuum,

the residue and *meso*-ferrocenyl dipyrromethane (0.07 g, 0.20 mmol) were dissolved in ethanol (15 mL). The mixture was then treated with Zn(OAc)₂ (0.37 g, 2 mmol) and refluxed open to air for 12 h. After removal of the solvent, the residue was chromatographed on neutral alumina to afford a green-colored solid which was identified as **8**. Yield: 0.04 g, 19%. Mp: 235–237 °C (dec.). Anal. Calcd. for C₆₃H₄₃CoFeN₄Zn: C, 73.02; H, 4.18; N, 5.41. Found: C, 73.09; H, 4.11; N, 5.39. ¹H NMR (δ , 300 MHz, CDCl₃): 4.23 (5H, s, Cp Fc), 4.80 (2H, s, Cp Fc), 5.26 (2H, s, Cp), 5.48 (2H, s, Cp Fc), 5.94 (2H, s, Cp), 6.71–7.27 (20H, m, PhH), 8.57 (2H, d, ³J = 4.2 Hz), 9.03 (2H, d, ³J = 4.2 Hz), 9.61 (2H, s), 9.64 (2H, d, ³J = 4.2 Hz), 10.14 (2H, d, ³J = 4.2 Hz). UV/vis (CH₂Cl₂); λ_{max} nm (log ϵ , M⁻¹ cm⁻¹) 422 (4.92), 561 (3.71), 624 (3.44). MS: Calcd. for C₆₃H₄₃CoFeN₄Zn: 1034.1461, Found: 1034.1605.

Synthesis of the Demetalated Porphyrin 9. **8** (0.10 g, 0.10 mmol) was dissolved in 10 mL of dichloromethane and the solution was stirred for 10 min. Then 0.03 mL of trifluoroacetic acid was added and the mixture was stirred for 1 h. The reaction mixture was neutralized by addition of triethylamine 0.02 mL, and reaction mixture was washed with brine and then with water. The organic layer was dried over anhydrous sodium sulfate, and the solvent was removed under reduced pressure. The resulting viscous dark green colored solid was chromatographed through neutral alumina using 5% ethyl acetate/hexane as eluent to give a green crystalline solid which was identified as **9** Yield: 0.05 g, 53%. Mp: 235–238 °C (dec.). Anal. Calcd. for C₆₃H₄₅CoFeN₄Zn: C, 77.78; H, 4.66; N, 5.76. Found: C, 77.69; H, 4.74; N, 5.70. ¹H NMR (δ , 300 MHz, CDCl₃): -1.99 (1H, s, br), -1.92 (1H, s, br), 4.30 (5H, s, Cp), 4.88 (2H, s, Cp Fc), 5.28 (2H, s, Cp), 5.63 (2H, s, Cp Fc), 5.98 (2H, s, Cp), 6.84–7.36 (20H, m, PhH), 8.84 (2H, d, ³J = 4.5 Hz), 9.28 (2H, d, ³J = 4.8 Hz), 9.54 (2H, d, ³J = 4.2 Hz), 10.00 (2H, s), 10.10 (2H, d, ³J = 4.5 Hz). UV/vis (CH₂Cl₂); λ_{max} nm (log ϵ , M⁻¹ cm⁻¹) 417 (4.50), 596 (3.66), 672 (3.63). HRMS: Calcd. for C₆₃H₄₆CoFeN₄: 973.2404, Found: 973.2333.

Synthesis of Compound 10. η^5 -[C₅H₄(CHO)]Co(η^4 -C₄Ph₄) (0.10 g, 0.19 mmol) and 5-(pentafluorophenyl) dipyrromethane (0.06 g, 0.18 mmol) were dissolved in (16 mL) at room temperature in the dark before trifluoroacetic acid (2.00 mg, 0.02 mmol) was added to initiate the condensation. The mixture was stirred for 12 h at room temperature, and the reaction was quenched with DDQ (0.06 g, 0.26 mmol). Stirring was continued for 1 h. Then triethylamine (1.60 mg, 0.02 mmol) was added to neutralize the acid. The solvents were removed under reduced pressure, and the resultant material was purified by column chromatography over neutral alumina using a 20% mixture of ethyl acetate/hexane as the eluent, to give a green-colored solid which was identified as the A₂B₂ type porphyrin **10**. Yield: (0.02 g, 14%) Mp: 227–229 °C (dec.). Anal. Calcd. for C₉₈H₅₈Co₂F₁₀N₄: C, 73.59; H, 3.66; N, 3.50. Found: C, 73.52; H, 3.71; N, 3.59. ¹H NMR (δ , 300 MHz, CDCl₃): -2.18 (2H, s, br), 5.22 (4H, s, Cp), 5.89 (4H, s, Cp), 6.74–7.64 (40H, m, Ph), 8.05 ((4H, d, ³J = 4.2 Hz), 9.38 (4H, d, ³J = 4.8 Hz). UV/vis (CH₂Cl₂); λ_{max} nm (log ϵ , M⁻¹ cm⁻¹) 423 (4.19), 616 (3.43), 681 (2.89). HRMS: Calcd. for C₉₈H₅₉Co₂F₁₀N₄: 1599.3244, Found: 1599.2924.

Synthesis of Compound 11. η^5 -[C₅H₄(CHO)]Co(η^4 -C₄Ph₄) (0.25 g, 0.50 mmol) and 5-(mesityl)dipyrromethane (0.13g, 0.50 mmol) were dissolved in 35 mL of dichloromethane at room temperature in dark before trifluoroacetic acid (4.00 mg, 0.04 mmol) was added to initiate the condensation. The mixture was stirred for 12 h at room temperature, and the reaction was quenched with DDQ (0.15 g, 0.65 mmol). Stirring was continued for 1 h and triethylamine (2.4 mg, 0.02 mmol) was added to neutralize the acid. The solvents were removed under reduced pressure, and the resultant material was purified by column chromatography over neutral alumina using an ethyl acetate/hexane 10% mixture as the eluent, to give a green-colored solid which was identified as the A₂B₂ type porphyrin **11**. Yield: 0.06 g, 6% Mp: 237–239 °C (dec.). Anal. Calcd. for C₁₀₄H₈₀Co₂N₄: C, 73.07; H, 4.74; N, 3.22. Found: C, 73.11; H, 4.63; N, 3.25. ¹H NMR (δ , 300 MHz, CDCl₃): -1.80 (2H, s, br), 1.77 (12H, s, CH₃), 2.66 (6H, s, CH₃), 5.15 (4H, s, Cp), 5.93 (4H, s, Cp), 6.80–7.45 (46H, m, Ph), 8.04 (4H, d, ³J = 4.5 Hz), 9.36 (4H, d, ³J = 4.5 Hz). UV/vis (CH₂Cl₂); λ_{max} nm (log ϵ , M⁻¹ cm⁻¹) 443 (4.91),

610 (4.30), 698 (4.12). HRMS: Calcd. for $C_{104}H_{80}Co_2N_4$: 1502.5047, Found: 1599.2924.

Synthesis of Compounds 12 and 13. η^5 -[$C_3H_4(CHO)$]Co(η^4 - C_4Ph_4) (0.25 g, 0.50 mmol) and 4-*tert*-butylphenyldiopyromethane (0.14 g, 0.50 mmol) were dissolved in (35 mL) at room temperature in the dark before trifluoroacetic acid (4.00 mg, 0.04 mmol) was added to initiate the condensation. The mixture was stirred for 12 h at room temperature, the reaction was quenched with DDQ (0.15 g, 0.65 mmol). Stirring was continued for 1 h, and triethylamine (2.4 mg, 0.02 mmol) was added to neutralize the acid. The solvents were removed under reduced pressure, and the resultant material was purified by column chromatography over neutral alumina using an ethyl acetate/hexane 2% mixture as the eluent, to give a green-colored solid identified as the AB₃ type 12. Yield: 0.01 g, 3%. Mp: 235–238 °C (dec.). Anal. Calcd. for $C_{83}H_{73}CoN_4$: C, 84.10; H, 6.21; N, 4.73. Found: C, 84.22; H, 6.14; N, 4.81. ¹H NMR (δ , 300 MHz, CDCl₃): -2.47 (2H, s, br), 1.57 (27H, s, CH₃), 5.22 (2H, s, Cp), 5.92 (2H, s, Cp), 6.77–7.45 (20H, m, Ph), 7.75 (6H, m), 8.07 (6H, m), 8.79 (6H, m), 9.44 (2H, s, ³J = 4.5 Hz). UV/vis (CH₂Cl₂); λ_{max} nm (log ϵ , M⁻¹ cm⁻¹) 423 (4.15), 581 (3.08), 665 (2.93). MS: Calcd. for $C_{83}H_{74}CoN_4$: 1185.5245, Found: 1185.5143. Further on elution using ethyl acetate/hexane 5% mixture gave another green solid which was identified as the *cis*-A₂B₂ type porphyrin 13. Yield: (0.015 g, 4%). Mp: 235–238 °C (dec.). Anal. Calcd. for $C_{106}H_{84}Co_2N_4$: C, 83.12; H, 5.53; N, 3.66. Found: C, 83.16; H, 5.63; N, 3.62. ¹H NMR (δ , 300 MHz, CDCl₃): -2.35 (2H, s, br), 1.49 (18H, s, CH₃), 5.14 (4H, s, Cp), 5.75 (4H, s, Cp), 6.5–7.25 (40H, m, Ph), 7.54 (4H, m), 7.98 (4H, m), 8.28 (2H, m), 8.65 (2H, m), 8.84 (2H, m), 9.19 (2H, m). UV/vis (CH₂Cl₂); λ_{max} nm (log ϵ , M⁻¹ cm⁻¹) 443 (4.75), 612 (4.15), 682 (4.03). MS: Calcd. for $C_{106}H_{85}Co_2N_4$: 1531.5438, Found: 1531.4621.

■ ASSOCIATED CONTENT

Supporting Information

Tables of selected bond lengths and angles and crystallographic information files (CIF) for compounds 1, 2, 3, 4, 5, 7, 9, 11, and 13. This material is available free of charge via the Internet at <http://pubs.acs.org>.

■ AUTHOR INFORMATION

Corresponding Author

*E-mail: eliasanil@gmail.com.

Notes

The authors declare no competing financial interest.

■ ACKNOWLEDGMENTS

The authors thank the Department of Science and Technology (DST), India, and CSIR India for financial assistance in the form of research grants to A.J.E. [DST SR/SI/IC-43/2010 and CSIR 01(2693)/12/EMR-II]. K.K. thanks CSIR India for a research fellowship. We dedicate this paper to Prof. T.K. Chandrashekar, FNA, India, whose pioneering work on ferrocenyldiopyromethane (ref 6) has been the inspiration for carrying out this work. We thank DST-FIST and IITD for funding of the single crystal X-ray diffraction and HRMS facilities at IIT Delhi.

■ REFERENCES

(1) (a) Bucher, C.; Devillers, C. H.; Moutet, J.-C.; Royal, G.; Saint-Aman, E. *Coord. Chem. Rev.* **2009**, *253*, 21–36. (b) Shoji, O.; Okada, S.; Satake, A.; Kobuke, Y. *J. Am. Chem. Soc.* **2005**, *127*, 2201–2210. (c) Bucher, C.; Devillers, C. H.; Moutet, J.-C.; Royal, G.; Saint-Aman, E. *Chem. Commun.* **2003**, 888–889. (d) Bucher, C.; Devillers, C. H.; Moutet, J.-C.; Royal, G.; Saint-Aman, E. *New J. Chem.* **2004**, *28*, 1584–1589.

(2) Suijkerbuijk, B. M. J. M.; Gebbink, R. J. M. *Angew. Chem., Int. Ed.* **2008**, *47*, 7396–7421.

(3) (a) Gryko, D. T.; Zhao, F.; Yasser, A. A.; Roth, K. M.; Bocian, D. F.; Kuhr, W. G.; Lindsey, J. S. *J. Org. Chem.* **2000**, *65*, 7356–7362. (b) Wei, L.; Padmaja, K.; Youngblood, W. J.; Lysenko, A. B.; Lindsey, J. S.; Bocian, D. F. *J. Org. Chem.* **2004**, *69*, 1461–1469. (c) Ambroise, A.; Wagner, R. W.; Rao, P. D.; Riggs, J. A.; Hascoat, P.; Diers, J. R.; Seth, J.; Lamm, R. K.; Bocian, D. F.; Holten, D.; Lindsey, J. S. *Chem. Mater.* **2001**, *13*, 1023–1034.

(4) (a) Nemykin, V. N.; Rohde, G. T.; Barrett, C. D.; Hadt, R. G.; Bizzarri, C.; Galloni, P.; Floris, B.; Nowik, I.; Herber, R. H.; Marrani, A. G.; Zanon, R.; Loim, N. M. *J. Am. Chem. Soc.* **2009**, *131*, 14969–14978. (b) Nemykin, V. N.; Rohde, G. T.; Barrett, C. D.; Hadt, R. G.; Sabin, J. R.; Reina, G.; Galloni, P.; Floris, B. *Inorg. Chem.* **2010**, *49*, 7497–7509.

(5) Wollmann, R. G.; Hendrickson, D. N. *Inorg. Chem.* **1977**, *16*, 3079–3089.

(6) (a) Narayanan, S. J.; Venkatraman, S.; Dey, S. R.; Sridevi, B.; Anand, V. R. G.; Chandrashekar, T. K. *Synlett* **2000**, 1834–1836. (b) Venkatraman, S.; Prabhuraja, V.; Mishra, R.; Kumar, R.; Chandrashekar, T. K.; Teng, W. J.; Senge, K. R. *Indian J. Chem.* **2003**, *42*, 2191–2197.

(7) Bakar, M. A.; Sergeeva, N. N.; Juillard, T.; Senge, M. O. *Organometallics* **2011**, *30*, 3225–3228.

(8) (a) Shetti, V. S.; Ravikanth, M. *Eur. J. Org. Chem.* **2010**, 494–508. (b) Lakshmi, V.; Santosh, G.; Ravikanth, M. *J. Organomet. Chem.* **2011**, *696*, 925–931. (c) Rai, S.; Gayatri, G.; Sastry, G. N.; Ravikanth, M. *Chem. Phys. Lett.* **2008**, *467*, 179–185.

(9) (a) Kalita, D.; Morisue, M.; Kobuke, Y. *New J. Chem.* **2006**, *30*, 77–92. (b) Morisue, M.; Kalita, D.; Haruta, N.; Kobuke, Y. *Chem. Commun.* **2007**, 2348. (c) Nakagawa, H.; Ogawa, K.; Satake, A.; Kobuke, Y. *Chem. Commun.* **2006**, 1560–1562.

(10) (a) D'Souza, F.; Smith, P. M.; Gadde, S.; McCarty, A. L.; Kullman, M. J.; Zandler, M. E.; Itou, M.; Araki, Y.; Ito, O. *J. Phys. Chem. B* **2004**, *108*, 11333–11343. (b) D'Souza, F.; Chitta, R.; Gadde, S.; Islam, D.-M. S.; Schumacher, A. L.; Zandler, M. E.; Araki, Y.; Ito, O. *J. Phys. Chem. B* **2006**, *110*, 25240–25250.

(11) (a) Poon, K.-W.; Liu, W.; Chan, P.-K.; Yang, Q.; Chan, T.-W. D.; Mak, T. C. W.; Ng, D. K. P. *J. Org. Chem.* **2001**, *66*, 1553–1559. (b) Cheng, K.-L.; Li, H.-W.; Ng, D. K. P. *J. Organomet. Chem.* **2004**, *689*, 1593–1598. (c) Schmidt, E. S.; Calderwood, T. S.; Bruce, T. C. *Inorg. Chem.* **1986**, *25*, 3718–3720.

(12) (a) Nakamura, A.; Hagihara, N. *Bull. Chem. Soc. Jpn.* **1961**, *34*, 452. (b) Boston, J. L.; Sharp, D. W. A.; Wilkinson, G. *J. Chem. Soc.* **1962**, 3488. (c) MacFarland, D. K.; Gorodtzer, R. *J. Chem. Educ.* **2005**, *82*, 109–110. (d) Harcourt, E. M.; Yonis, S. R.; Lynch, D. E.; Hamilton, D. G. *Organometallics* **2008**, *27*, 1653–1656.

(13) (a) Rausch, M. D.; Genetti, R. A. *J. Org. Chem.* **1970**, *35*, 3888–3897. (b) Rausch, M. D. *Pure Appl. Chem.* **1972**, *30*, 528. (c) Helling, J. F.; Rennison, S. C.; Merijon, A. *J. Am. Chem. Soc.* **1967**, *89*, 7140–7141. (d) Wakatsuki, Y.; Yamazaki, H. *Inorg. Synth.* **1989**, *26*, 189–200.

(14) (a) Singh, N.; Elias, A. J. *Organometallics* **2012**, *31*, 2059–2065. (b) Singh, N.; Elias, A. J. *Dalton. Trans.* **2011**, *40*, 4882–4891. (c) Rajkumar, J.; Kumar, M. S.; Singh, N.; Elias, A. J. *J. Organomet. Chem.* **2008**, *693*, 3780–3786. (d) Kumar, M. S.; Upreti, S.; Elias, A. J. *Inorg. Chem.* **2006**, *45*, 7835–7842. (e) Singh, N.; Metla, B. P. R.; Elias, A. J. *J. Organomet. Chem.* **2012**, *717*, 99–107. (f) Mandapati, P.; Singh, N.; Kumar, D.; Elias, A. J. *J. Organomet. Chem.* **2012**, *716*, 208–215.

(15) (a) Nomura, H.; Richards, C. J. *Chem. Asian J.* **2010**, *5*, 1726–1740. (b) Nguyen, H. V.; Yeamine, M. R.; I, Amin, J.; Motevalli, M.; Richards, C. J. *J. Organomet. Chem.* **2008**, *693*, 3668–3676. (c) Nomura, H.; Richards, C. J. *Chem.—Eur. J.* **2007**, *13*, 10216–10224. (d) Yeamine, M. R.; Richards, C. J. *Tetrahedron: Asymmetry* **2007**, *18*, 2613–2616. (e) Jones, G.; Richards, C. J. *Organometallics* **2001**, *20*, 1251–1254. (f) Prasad, R. S.; Anderson, C. E.; Richards, C. J.; Overman, L. E. *Organometallics* **2005**, *24*, 77–81. (g) Overman, L.

- E.; Owen, C. E.; Pavan, M. M.; Richards, C. J. *Org. Lett.* **2003**, *5*, 1809–1812.
- (16) (a) Bertrand, G.; Tortech, L.; Fichou, D.; Malacria, M.; Aubert, C.; Gandon, V. *Organometallics* **2012**, *31*, 126–132. (b) Geny, A.; Agnet, N.; Iannazzo, L.; Malacria, M.; Aubert, C.; Gandon, V. *Angew. Chem., Int. Ed.* **2009**, *48*, 1810–1813.
- (17) (a) Courtney, D.; McAdam, C. J.; Manning, A. R.; Mueller-Bunz, H.; Ortin, Y.; Simpson, J. J. *Organomet. Chem.* **2012**, *705*, 7–22. (b) O'Donohue, P.; Brusey, A.; Seward, C. M.; Ortin, Y.; Molly, B. C.; Mueller-Bunz, H.; Manning, A. R.; McGlinchey, M. J. *J. Organomet. Chem.* **2009**, *694*, 2536–2547. (c) Kjaergaard, H. G.; McAdam, C.; John, M.; Anthony, R.; Mueller-Bunz, H.; O'Donohue, P.; Ortin, Y.; Robinson, B. H.; Simpson, J. *Inorg. Chim. Acta* **2008**, *361*, 1616–1623.
- (18) (a) Anderson, C. E.; Overman, L. E.; Richards, C. J.; Watson, M. P.; White, N. *Org. Synth.* **2007**, *84*, 139–147. (b) Anderson, C. E.; Overman, L. E. *J. Am. Chem. Soc.* **2003**, *125*, 12412–12413. (c) Ghosh, A. K.; Mathivanan, P.; Cappiello, J. *Tetrahedron: Asymmetry* **1998**, *9*, 1–45. (d) Aubert, C.; Bertrand, G.; Fichou, D.; Gandon, V.; Malacria, M.; Torten, L. *Fr. Demande*, FR 2973574 A1 20121005, 2012. (e) Aubert, C.; Bertrand, G.; Fichou, D.; Gandon, V.; Malacria, M.; Torten, L. *Fr. Demande*, FR 2973379 A1 20121005, 2012. (f) Dabek, S.; Proscenc, M. H.; Heck, J. *Organometallics* **2012**, *31*, 6911–6925.
- (19) (a) Loim, N. M.; Abramova, N. V.; Khaliullin, R. Z.; Lukashov, Y. S.; Vorontsov, E. V.; Sokolov, V. I. *Russ. Chem. Bull.* **1998**, *47*, 1045–1049. (b) Loim, N. M.; Abramova, N. V.; Khaliullin, R. Z.; Sokolov, V. I. *Russ. Chem. Bull.* **1997**, *46*, 1193–1194. (c) Loim, N. M.; Kondratenko, M. A.; Grishko, E. V.; Sokolov, V. I. *Russ. Chem. Bull.* **1994**, *43*, 905–906. (d) Loim, N. M.; Grishko, E. V.; Pyshnograeva, N. I.; Vorontsov, E. V.; Sokolov, V. I. *Russ. Chem. Bull.* **1994**, *43*, 871–873.
- (20) Gallagher, J. F.; Moriarty, E. *Acta Crystallogr. Sect. C* **1999**, *55*, 1079–1082.
- (21) Ryppa, C.; Senge, M. O.; Hatscher, S. S.; Kleinpeter, E.; Wacker, P.; Schilde, U.; Wiehe, A. *Chem.—Eur. J.* **2005**, *11*, 3427–3442.
- (22) Wiehe, A.; Ryppa, C.; Senge, M. O. *Org. Lett.* **2002**, *4*, 3807–3809.
- (23) Zhang, L.; Qi, D.; Zhang, Y.; Bian, Y.; Jiang, J. *J. Mol. Graph. Mod.* **2010**, *29*, 717–725.
- (24) Taniguchi, M.; Balakumar, A.; Fan, D.; McDowell, B. E.; Lindsey, J. S. *J. Porphyrins Phthalocyanines* **2005**, *9*, 554–574.
- (25) Bhaumik, J.; Yao, Z.; Borbas, E.; Taniguchi, M.; Lindsey, J. S. *J. Org. Chem.* **2006**, *71*, 8807–8817.
- (26) Kumar, M. S.; Upreti, S.; Gupta, H. P.; Elias, A. J. *J. Organomet. Chem.* **2006**, *691*, 4708–4716.
- (27) Littler, B. J.; Ciringh, Y.; Lindsey, J. S. *J. Org. Chem.* **1999**, *2864*–2872.
- (28) Madhu, s.; Ravikanth, M. *Inorg. Chem.* **2012**, *51*, 4285–4292.
- (29) Kee, H. L.; Kirmaier, C.; Tang, Q.; Diers, J. R.; Muthiah, C.; Taniguchi, M.; Laha, J. K.; Ptaszek, M.; Lindsey, J. S.; Bocian, D. F.; Holten, D. *Photochem. Photobiol.* **2007**, *83*, 1125–1143.
- (30) Auger, A.; Swarts, J. C. *Organometallics* **2007**, *26*, 102–109.
- (31) Auger, A.; Muller, A. J.; Swarts, J. C. *Dalton. Trans.* **2007**, 3623–3633.
- (32) (a) Jentzen, W.; Simpson, M. C.; Hobbs, J. D.; Song, X.; Ema, T.; Nelson, N. Y.; Medforth, C. J.; Smith, K. M.; Veyrat, M.; Mazzanti, M.; Ramasseu, R.; Marchon, J.-C.; Takeuchi, T.; Goddard, W. A.; Shelnutt, J. A. *J. Am. Chem. Soc.* **1995**, *117*, 11085–11097. (b) Juillard, S.; Ferrand, Y.; Simonneaux, G.; Toupet, L. *Tetrahedron* **2005**, *61*, 3489–3495. (c) Saltsman, I.; Goldberg, I.; Balasz, Y.; Gross, Z. *Tetrahedron Lett.* **2007**, *48*, 239–244.
- (33) Rausch, M. D.; Higbie, F. A.; Westover, G. F.; Clearfield, A.; Gopal, R.; Troup, J. M.; Bernal, I. J. *Organomet. Chem.* **1978**, *149*, 245–264.
- (34) Senge, M. O. *Chem. Commun.* **2006**, 243–256.
- (35) Li, M.; Yao, Y.-M.; Zou, J.-Z.; Xu, Z.; You, X.-Z. *Chin. J. Chem.* **1994**, *12*, 237–242.
- (36) (a) Rhee, S. W.; Na, Y. H.; Do, Y.; Kim, J. *Inorg. Chim. Acta* **2000**, *309*, 49–56. (b) Rhee, S. W.; Park, B. B.; Do, Y.; Kim, J. *Polyhedron* **2000**, *19*, 1961–1966. (c) Boyd, P. D. W.; Burrell, A. K.; Campbell, W. M.; Cocks, P. A.; Gordon, K. C.; Jameson, G. B.; Officer, D. L.; Zhao, Z. *Chem. Commun.* **1999**, 637–638.
- (37) Rai, S.; Gayatri, G.; Sastry, G. N.; Ravikanth, M. *Chem. Phys. Lett.* **2008**, *467*, 179–185.
- (38) O'Donohue, P.; McAdam, C. J.; Courtney, D.; Ortin, Y.; Müller-Bunz, H.; Manning, A. R.; McGlinchey, M. J.; Simpson, J. J. *Organomet. Chem.* **2011**, *696*, 1510–1527.
- (39) Koszarna, B.; Butensch, H.; Gryko, D. T. *Org. Biomol. Chem.* **2005**, *3*, 2640.
- (40) Hart, W. P.; Shihua, D.; Rausch, M. D. *J. Organomet. Chem.* **1985**, *282*, 111–121.
- (41) Wakatsuki, Y.; Yamazaki, H. *Inorg. Synth.* **1989**, *26*, 189–200.
- (42) Zhang, C.; Long, H.; Zhang, W. *Chem. Commun.* **2012**, *48*, 6172–6174.
- (43) Lee, M. J.; Seo, K. D.; Song, H. M.; Kang, M. S.; Eom, Y. K.; Kang, H. S.; Kim, H. K. *Tetrahedron Lett.* **2011**, *52*, 3879–3882.
- (44) (a) SMART: Bruker Molecular Analysis Research Tools, version 5.618; Bruker Analytical X-ray Systems: Madison, WI, 2000. (b) Sheldrick, G. M. SAINT-NT, version 6.04; Bruker Analytical X-ray Systems: Madison, WI, 2001. (c) Sheldrick, G. M. SHELXTL-NT, version 6.10; Bruker Analytical X-ray Systems: Madison, WI, 2000. (d) Klaus, B. DIAMOND, version 2.1c; University of Bonn: Bonn, Germany, 1999.